CONSTITUTIVE RELATIONS OF COAL AND COAL MEASURE ROCKS.

DRYING SHRINKAGE AND CREEP BEHAVIOR OF COAL

by

R. J. Tocher and H. Y. Ko

Prepared for

UNITED STATES DEPARTMENT OF INTERIOR
BUREAU OF MINES

by

UNIVERSITY OF COLORADO
DEPARTMENT OF CIVIL, ENVIRONMENTAL,
AND ARCHITECTURAL ENGINEERING
BOULDER, COLORADO 80309

Bureau of Mines Open File Report 54(3)-83

FINAL REPORT OF INVESTIGATIONS
VOLUME 3

Supported by
Grant No. G0155056
(Constitutive Relations of Coal and Coal Measure Rocks)
Hon-Yim Ko and Kurt H. Gerstle, Principal Investigators

March 1980

50272-101

REPORT DOCUMENTATION PAGE	1. REPORT NO. BuMines OFR 54(3)-83	2.	3. Recipient's Accession No. PB83 178269
4. Title and Subtitle: Constitutive Relations of Coal and Coal Measure Rocks. Volume III. Drying Shrinkage and Creep Behavior of Coal			5. Report Date: Mar. 1980
7. Author(s): R. J. Tocher and H. Y. Ko			8. Performing Organization Rept. No.
9. Performing Organization Name and Address: University of Colorado, Department of Civil, Environmental and Architectural Engineering, Boulder, CO 80309			10. Project/Task/Work Unit No.
			11. Contract(C) or Grant(G) No. (C) (G) G0155056
12. Sponsoring Organization Name and Address: Office of Assistant Director--Mining Research, Bureau of Mines, U.S. Department of the Interior, Washington, DC 20241			13. Type of Report & Period Covered: University grant, 1/1/75--2/28/80
			14.

15. Supplementary Notes

Approved for release February 16, 1983.

16. Abstract (Limit: 200 words)

Uniaxial testing was performed on coal specimens to determine the time-dependent response. The testing was carried out on coal from six mine sites throughout the Western United States and Pennsylvania. Testing configurations were varied to allow analysis of moisture dependency, stress level, and specimen orientation. Several theories were presented for the behavior of coal due to moisture diffusion. Experimental results showed the correlation between the theories and the actual material response. Coal deformation was found to be highly dependent on the moisture level of the testing environment. Moisture migration causes drying and shrinkage which lead to progressive degradation of the material. The coal tested experienced a rebound if saturated after a period of drying. This type of time-dependent behavior overshadows the dependence on the applied stress level, which, however, still produces a noticeable creep behavior. Analysis of one series of creep test results was performed. A relationship was developed on the basis of a simplified rheological model to describe the coal response to uniaxial stress. Previous empirical formulations in the form of power laws were compared and their deficiencies pointed out.

17. Document Analysis a. Descriptors

Mining
Coal
Time dependent strain
Creep
Drying shrinkage
Rheology

b. Identifiers/Open-Ended Terms

c. COSATI Field/Group 08I

18. Availability Statement	19. Security Class (This Report)	21. No. of Pages
Release unlimited by NTIS	Unclassified	114
	20. Security Class (This Page) Unclassified	22. Price

(See ANSI-Z39.18) See Instructions on Reverse

OPTIONAL FORM 272 (4-77) (Formerly NTIS-35) Department of Commerce

DISCLAIMER NOTICE

The views and conclusions contained in this document are those of the author and should not be interpreted as necessarily representing the official policies or recommendations of the Interior Department's Bureau of Mines or of the U.S. Government.

-FORWARD-

This report was prepared by the University of Colorado, Department of Civil, Environmental, and Architectural Engineering under USBM Grant Number G01550156. The contract was initiated under the Coal Mine Health and Safety Program. It was administered under the technical direction of Denver Mining Research Center with Dr. L. A. Panek acting as the Technical Project Officer. Mr. A. G. Young was the contract administrator for the Bureau of Mines.

This report is a summary of the work recently completed as part of this contract during the period January 1, 1975 to February 28, 1980. This report was submitted by the authors on March 1, 1980.

TABLE OF CONTENTS

CHAPTER I

INTRODUCTION

Purpose

The analysis of the time dependent behavior of structural systems such as coal mines is based on obtaining mathematical solutions to stresses and strains while taking into account equilibrium, boundary conditions and stress-strain relations. Prior to the extensive use of numerical methods many simplifications in complex geometries had to be made to obtain analytical solutions.

With such numerical techniques as the finite element method, it is frequently possible to solve for the time dependent stress and strain distributions of structures with complex geometries and material properties such as coal mines. By using the experimentally obtained behavior of the coal as the material behavior input for numerical techniques, the time dependent response of a complex structure can be found.

The purpose of this investigation is to obtain the time dependent response of coal due to both applied stresses and drying shrinkage. The experimental behavior that is obtained is used to validate proposed theories of the creep behavior of coal. The mathematical models that are derived can then be used to predict the time dependent deformation and failure of coal mine openings.

1.2 Survey of Previous Work

1.2.1 Creep Testing

The first modern investigation done on the creep of materials was by Andrade (1910) who performed experiments on lead, copper and alloy wires in tension. Andrade found that after a sufficiently long period of time the strain rate was approximately constant. He fitted the early section of the creep curve to

$$L_t - L_o = At^{1/3}$$

where

L_o = initial length

L_t = length at time t

A = A constant

and proposed the creep law

$$L_t = L_o\ (1 + Bt^{1/3})\ \exp^{(kt)} \qquad (2.2)$$

This expression can be reduced for small strains and short times to

$$L_t = L_o\ (1 + Bt^{1/3}) \qquad (2.3)$$

where B is constant. Andrade referred to creep behavior at short time periods as "β-creep" and to long term behavior as "viscous flow". Various authors have used other terms to describe these phases. β-creep has been called elastic, primary, transient, logarithmic, Andrade and α-creep. Viscous flow has been called pseudoviscous, secondary and steady-state creep. In this report the terms transient and steady-state will be used since they

have no implications as to the mechanism of creep or the form of the creep law and are generally accepted as the most common terms.

Griggs (1939) proposed the first creep laws based on experiments run on rocks. He proposed that the total creep strain be described as

$$e = A + B \text{ Log } t + C_t \tag{2.4}$$

The coefficients A and B were obtained by plotting the creep curve on semi-logarithmic paper. A straight line was drawn through the early values of e. The slope of the line was used to estimate B and the strain intercept was A. The straight line fitted to the earlier data was subtracted from the latter data and the differences plotted on ordinary graph paper. A straight line through the origin whose slope was e could then be fitted to the results.

Burger's model (Fig. 2.1) has been used by Hardy (1965) to obtain Equation (2.5),

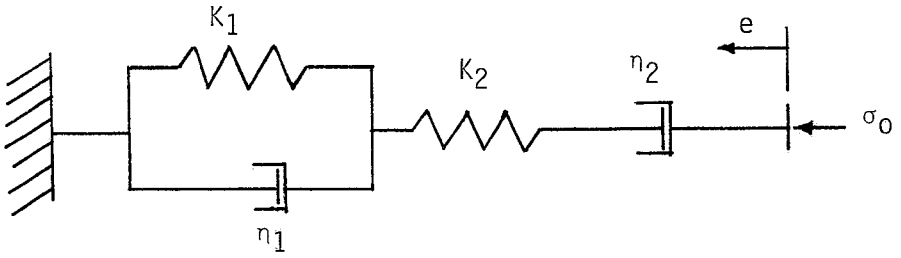

Figure 1.1 Burger's Rheological Model

$$e = \frac{\sigma_o}{K_1}\left[1 - e^{\frac{-Kt}{\eta_1}}\right] + \frac{\sigma_o}{K_2} + \frac{\sigma_o t}{\eta_2} \tag{2.5}$$

where σ_o/K_2 was the instantaneous elastic strain and $\sigma_o/K_1 \left[1 - e^{-Kt/\eta_1}\right]$ represented transient creep. The constants were determined from a loading and unloading creep test. The permanent deformation was $\sigma_o t/\eta_2$ and the amount of strain recovered under zero load was σ_o/K_1 . The coefficient K_1/η_1 can be determined from the form of the curve showing recovery under zero load. However, experimental results obtained by Hardy did not correlate with the rheological model.

Other authors, Matsushima (1960) and Price (1964) have suggested logarithmic-creep laws and have obtained good correlation with experimental data.

Misra and Murrell (1965) have fitted a power function, $e = At^B$ to their data on the creep of salt. Different creep laws were used at different temperature ranges. At low temperatures, relative to the melting point, the creep was best described by $e = A + B \text{ Log } t$. Above one half the melting temperature the curves were approximated by $e = At^{1/3}$. In the transition zone between the two, a combined form of $e = A_1 + A_2 \text{ Log } t + A_3t^{B}1 + A_4t^{B}2$ proved suitable. Constants were estimated by the methods described by Griggs (1939). Winkel et al. (1972) have proposed a viscoplastic model to describe the creep of salt based on a rheological model.

Cruden (1971a, 1971b) analyzed the form of the creep law for rock under uniaxial compression, and compared the work of previous authors (Miska and Murrel, 1965; Price, 1964). He found that with a great variety of creep laws based on laboratory tests

it was difficult to get good agreement for creep values extrapolated to times of practical interest. Cruden divided his work into studying exponential laws and power laws. His method of analysis showed that the power law fit data more satisfactorily than the exponential laws without the addition of any component of steady-state creep.

During the Bureau of Mines sponsored project, "Constitutive Relations of Coal and Coal Measure Rocks" (Ko and Gerstle, 1974, 1976, 1977) at the University of Colorado, some empirical analysis of creep data has been performed. Tulin (Chapter 6, Ko and Gerstle, 1976) developed expressions for creep response based on the exponential law. He divided creep strains into different time domains to obtain the best correlation between experimental data and predicted behavior. However, no generalities were made and the significance of exponents was not discussed.

Several authors (Kidybinski, 1966; Terry and Morgans, 1958) have analyzed coal by developing more complex rheological models than Burger's model. Kidybinski (1966) developed a rheological model corresponding to plastic, elastic, visco-elastic and viscous strains. By connecting these models the behavior of the coal and coal measure rocks was found. Numerical values for the coefficients were also tabulated. Terry and Morgans (1958) studied elastic and time-dependent response of coal and modeled it rheologically. They proposed a series of springs and dashpots

coupled to a series chain of a large number of retardation elements covering a wide range of retardation times to best describe creep behavior.

1.2.2 Shrinkage Testing

Most of the work done to date on drying shrinkage has been concerned with clays, soil-cement slabs, and concrete (Haroon, 1974; Lorman, 1940; Power, 1965).

Analysis of rock deformability due to swelling and shrinkage has been performed only in recent years. Dragowski (1970) investigated the anisotropy of deformations during cyclic changes in water content. He found that the range of swelling and shrinkage deformations is related to the content of clay minerals, structures and texture of the rocks. The destructive action of the water cycling was manifested in the form of fissures. Kowalski (1974) showed how variations in water content result in differentiation of strength properties of rocks and accentuation of anisotropy. From this work it is shown that there is a definite need to consider shrinkage and strength softening in engineering considerations.

Several authors (Colback and Wiid, 1965; Huder and Sitar, 1975; Van Eeckhout and Peng, 1972; Wiid, 1970) have studied the mechanical properties of rocks and their relationship with moisture and shrinkage phenomena. Colback and Wild (1965) studied the relationship between moisture content and compressive strength and found that moisture decreased the strength of most rocks. Van Eeckhout and Peng (1972) investigated the relationship of

of elastic properties and moisture conditions in coal mine shales. They found that increased moisture decreased compliance values. Wiid (1970) showed how fracture initiation and unstable fracture propagation in rock are affected by moisture content.

1.3 Scope of Work

The investigation herein reported includes research into the following areas. The study is divided into two main parts; shrinkage behavior and creep behavior. Previous experimental data obtained during the Bureau of Mines sponsored project, "Constitutive Relations of Coal and Coal Measure Rocks" at the University of Colorado, is incorporated in the analysis of creep behavior.

In the first part, several test series are performed by the author on moist coals to analyze their drying behavior. The experimental results are then compared with proposed theories to provide validation.

The coal investigated in the creep studies is from six different mines in the United States: Big Horn Mine, Gillette, Wyoming; Bruceton U.S.B.M. Experimental Mine, Bruceton, Pennsylvania; Eagle Mine, Erie, Colorado; Lincoln Mine, Erie, Colorado; Orchard Valley Mine, Paonia, Colorado; and York Canyon Mine, Raton, New Mexico. All of the coals are characterized by bedding and cleat planes. The properties of these coals vary considerably and provide for good comparisons. All of the testing reported is uniaxial compression of NX size specimens. From the

experimental data base analytical and empirical relations are derived and compared with each series to get possible solutions to the creep behavior of coal.

CHAPTER 2

MATERIALS AND LABORATORY TESTING

2.1 Scope of Testing Program

This study is concerned with only uniaxial creep test results of coal. While some triaxial creep data is also available (Ko and Gerstle, 1977) it shows more scatter and does not cover all the ranges of variables and is therefore not considered. Long term uniaxial tests were performed on specimens ranging from 100 hours to 7,000 hours. Uniaxial stress levels from zero to 1,250 psi were used in the testing. Over the testing period of three years, 240 samples were tested from four mine sites.

2.2 Long Term Uniaxial Creep and Shrinkage Testing

All the uniaxial creep test results reported herein were obtained by the unconfined compression test on cylindrical specimens. All of the specimens used are NX size with a diameter of 2.129 inches and a length of 4.250 inches. Due to the tolerances of the sample preparation equipment the samples have a length of between 4.150 and 4.300 inches and a diameter of between 2.120 and 2.130 inches. The specimens were loaded axially in a frame as shown in Fig. 2.1. Axial strain and axial load are then measured at periodic intervals throughout the length of the test.

Several specimens can be stacked up and tested in the same frame as long as none of the samples fails prematurely. All measurements are made using mechanical deformation gauges with tolerances of ±0.0001 inches.

Equipment

A hydraulic jack is used to apply the axial load. Situated below the specimens is a calibrated aluminum proving ring used to obtain the exact load that is being transferred to the specimens. When the load applied to the specimen reaches the desired level, the upper plate is bolted down to constrain the specimen. The jack can then be removed and used to load other specimens. The large stiff spring is used to help keep the load approximately constant on the specimen as they deform. After some deformation of the specimen has occurred, the specimen relaxes and it becomes necessary to adjust the applied load by utilizing the jack again. The load is adjusted when the stress level falls below 90 percent of the desired value.

A .003 inch thick greased teflon sheet is placed on each end of the specimen. This is done to reduce the possibility of any shearing stresses developing on the ends of the specimen during the test. A spherical head as shown in Fig. 2.1 is used to transmit the load to the specimen thereby eliminating bending moments due to non-parallel end surfaces.

Axial deformation measurements are made with a mechanical dial gauge. Measurements are made between the guide plates on opposite sides of the specimen where grooves to hold the gauge

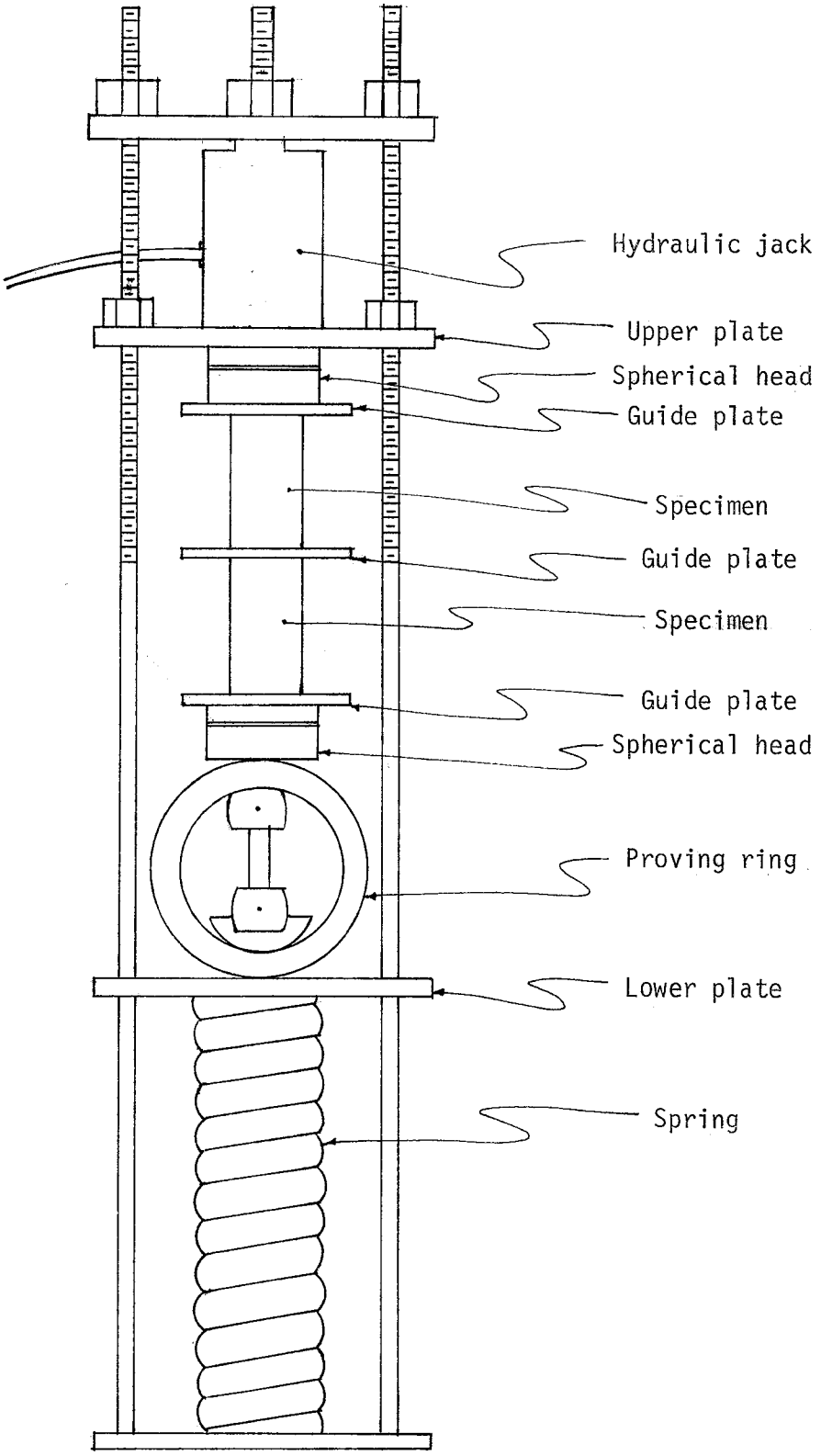

Figure 2.1 Uniaxial Test Set-up Used in Creep Studies

are located. The gauges measure to within ±0.0001 inches of the exact length. The measuring procedure is shown in Fig. 2.2.

A mechanical deformation Demac Gauge as shown in Fig. 2.3 is used to measure the load and calibrate the proving ring. The proving ring is calibrated by placing it in a Riehle Universal testing machine, applying incremental loads and measuring deflections. A linear relationship is found as shown in Fig. 2.4 for load vs. deflection. From this calibration curve the applied stress can be calculated.

Two types of specimens are used for the testing. One is unsealed, where no coating is used to prevent moisture evaporation from the surface of the specimen. The second type is a sealed specimen. The sealing in of the moisture is accomplished by either painting on a coat of impermeable "petrowax" or immersing the specimen in a water bath to prevent drying. The water bath is made by enclosing the sample loosely in a rubber membrane 2.8 inches in diameter and 7.0 inches long as shown in Fig. 2.5. The membrane is attached to platens above and below the specimen by rubber bands. The void between the sample and membrane is then filled with water from a squeeze bottle. The distinct advantage of the membrane over the wax is that the moisture migration potential can more easily be cycled.

Figure 2.6 shows the material and specimen reference systems. The material reference system is an orthogonal reference system which orients the bedding and cleat planes to a system of axes. The specimen reference system is an orthogonal coordinate

system used to orient the cylindrical uniaxial test specimens. The X direction is co-linear with the axis of the cylinder. The three angles α, β, and γ define the orientation of the specimen axis with respect to the material reference system.

2.3 Short-Term Uniaxial Testing

Short-term uniaxial testing is performed to determine approximate values of Young's Modulus and unconfined compressive strength. These tests are performed on the same NX size cylindrical specimens. The specimens are loaded axially by a hydraulic testing machine while measurements are made on axial strain and axial load. The test procedure is similar to that described in the preceding section for creep and shrinkage testing. Young's Modulus is then calculated as the slope of a line qualitatively drawn tangent to the linear portion of the stress-strain curve.

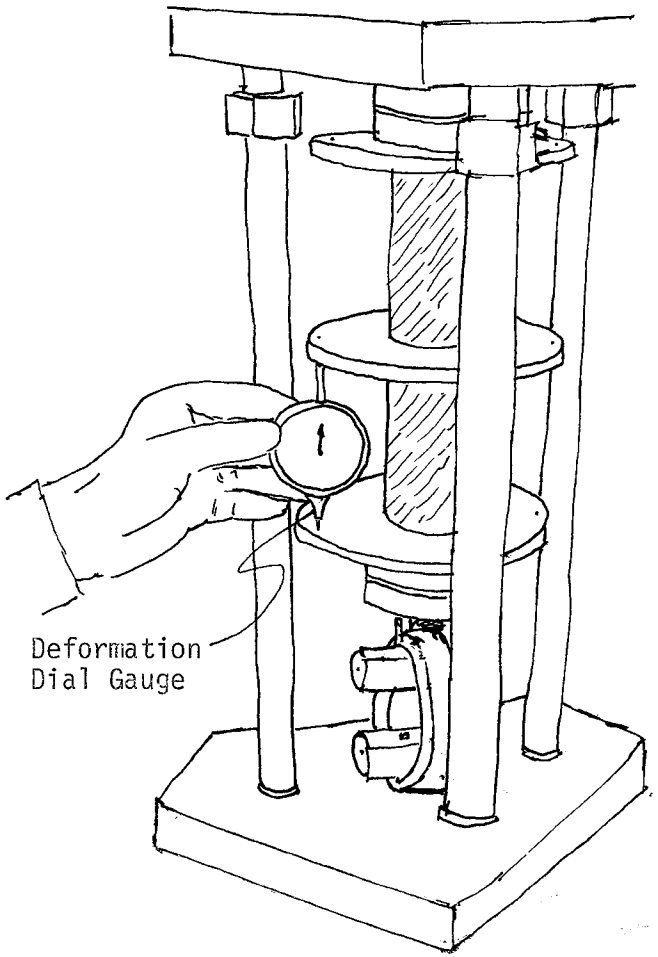

Figure 2.2 Strain Measurement

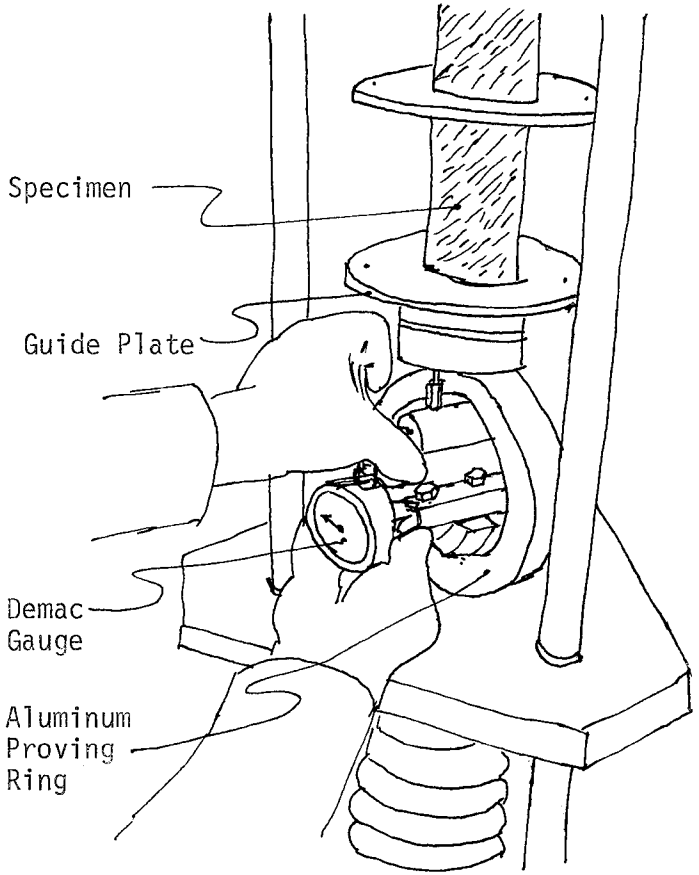

Figure 2.3 Stress Measurement

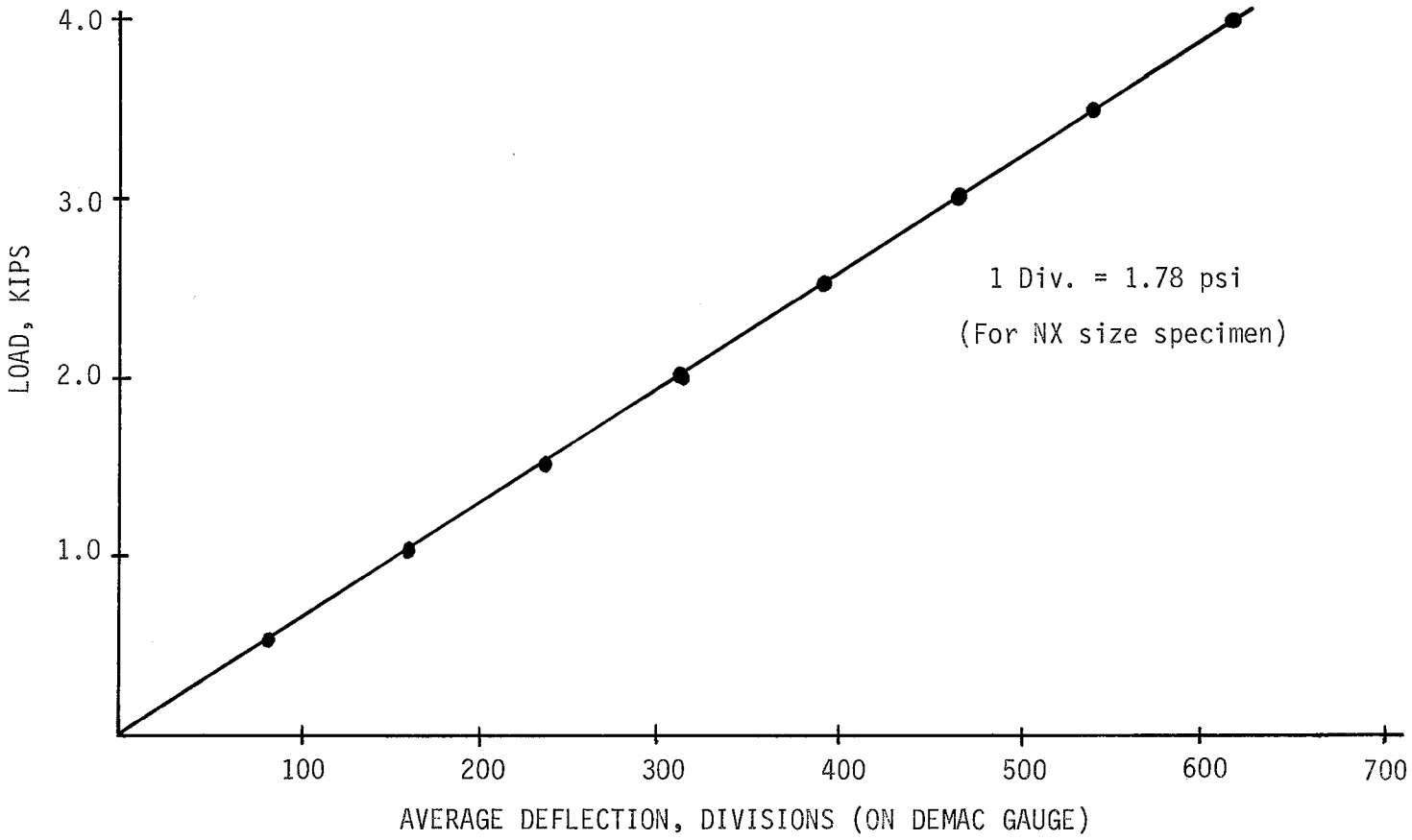

Figure 2.4 Aluminum Proving Ring Calibration Curve

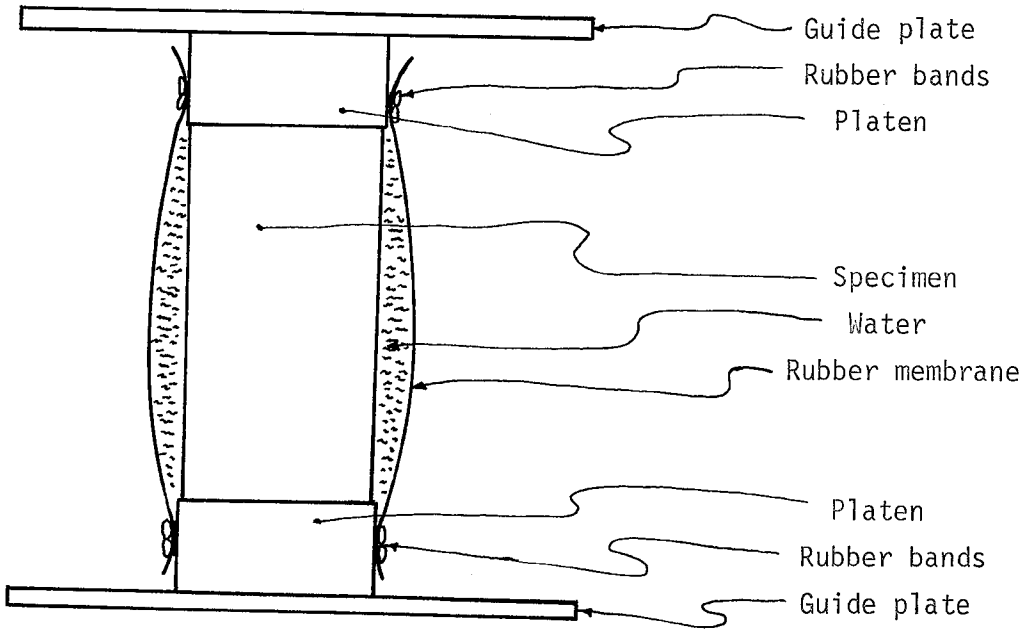

Figure 2.5 Specimen Sealed by a Water Bath in a Rubber Membrane

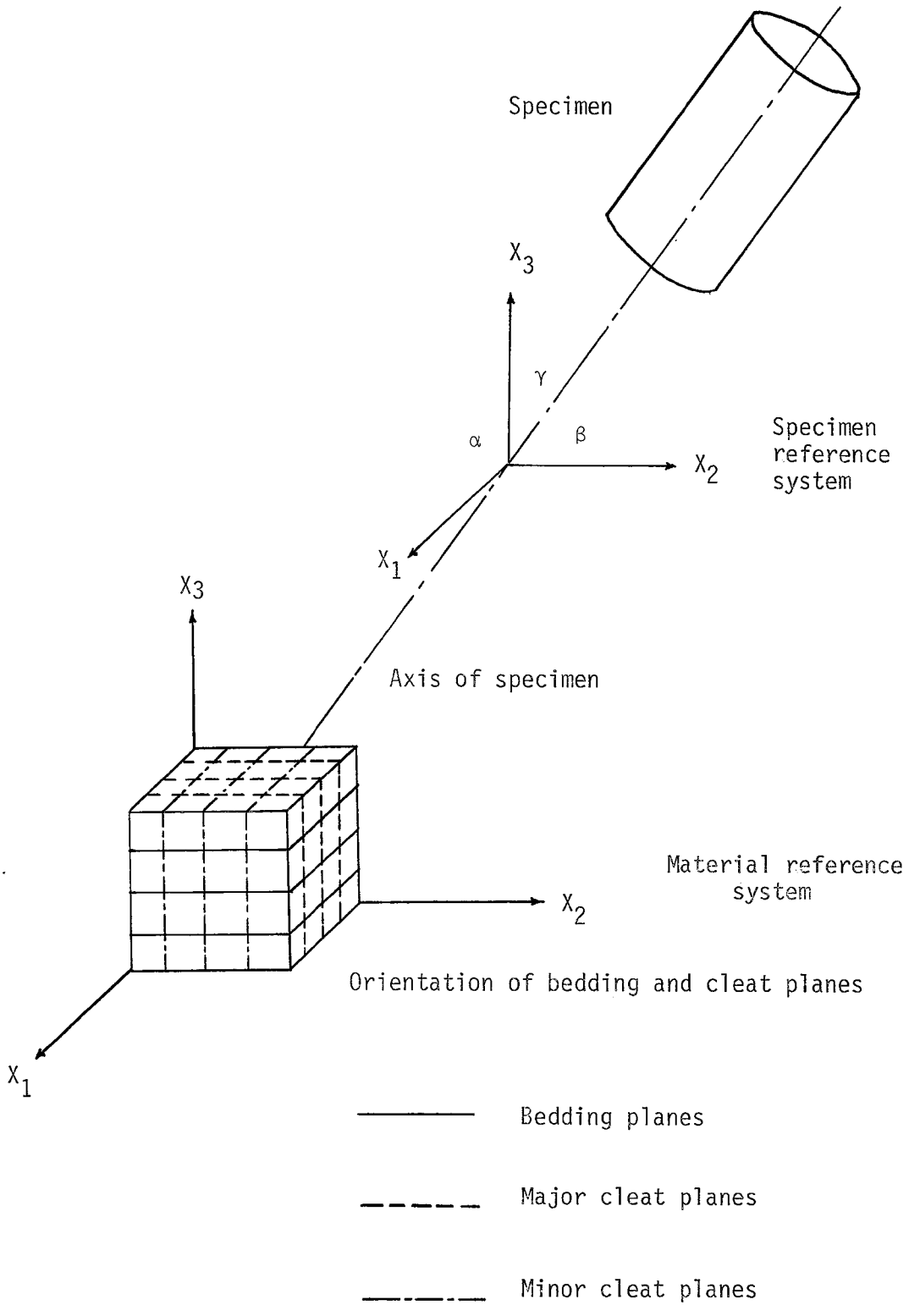

Figure 2.6 Specimen and Material Reference Systems

CHAPTER 3

MOISTURE DIFFUSION IN COAL

3.1 Introduction

The time-dependent strain of coal is partially due to the loss of moisture from the internal structure. The other significant portion of strain is due to applied stresses. For coals with higher moisture content strain related to moisture loss will be larger than for coals with a low moisture content. As water evaporates from the surface, the coal material becomes less saturated causing a more complex stress system to develop. This partially saturated material is analyzed in this chapter.

This chapter presents and analyzes different theories to explain the time-dependent response of several coal types to various stress and moisture conditions.

Previous work on the creep behavior of coal has been reported by Ko and Gerstle (1974, 1975, 1976, 1977) and is reproduced in Table 1 of Chapter 5. Results from these tests are incorporated in this report for an additional basis to support the theories presented. The following chapter presents experimental work performed by the author to demonstrate the theories presented in this chapter.

3.2 Proposed Theories of Behavior

3.2.1 Partial Saturation

Coal may be analyzed as a three-phase material, with the solid phase consisting of insoluble mineral particles forming a microstructure that is compressible. The second phase is liquid consisting of water which is incompressible. The third phase is gaseous having a mechanical response similar to that of air.

There are several relationships between weight and volume that describe the state of saturation and void ratio. These dimensionless quantities are expressed in terms of measurable quantities, water content (W), bulk mass specific gravity (G_M) and specific gravity of the solids (G_S).

The degree of saturation can be expressed as

$$S = \frac{W}{(1 + W)/G_M - 1/G_S} \tag{3.1}$$

or more simply

$$S = \frac{V_W}{V_V} \times 100 \tag{3.2}$$

where V_W = volume of water

and V_V = volume of voids

The void ratio can be expressed as

$$e = \frac{V_V}{V_S} = \frac{G_S\ (1 + W)}{G_M} - 1 \tag{3.3}$$

where V_S = volume of solids

Due to the varying compressibilities of the different phases of the system, the void geometry reacts to changes in

external and internal stresses. Values of void ratio and degree of saturation must be related to explicit values of external stress and time.

When the void space consists of both air and water the pore-water pressure U_W is always less than the pore-air pressure U_A, due to the development of surface tension. Assuming a low degree of saturation, the water will be present mainly as menisci in the vicinity of structural contacts as shown in Fig. 3.1. During the shrinkage straining of coal these menisci will develop.

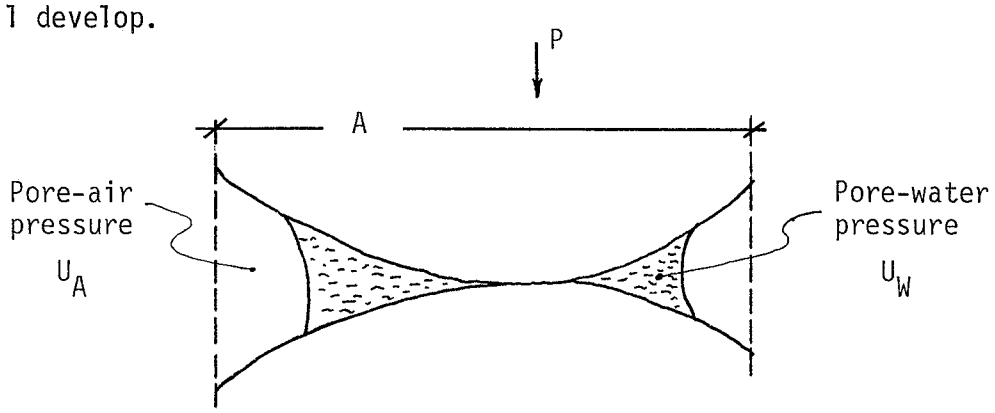

Figure 3.1 Stress in Structure due to Partial Saturation

By using the relationship for capillarity in a tube and relating it to a crack the surface tension can be found as follows:

$$T_S = \frac{h_c \gamma R}{2 \cos \alpha} \qquad (3.4)$$

where T_S = surface tension in the liquid

h_c = height of water in the crack

R = radius of crack at the meniscus

α = contact angle of the water and surface.

This is further discussed in the next section.

If the pore-water pressure acts over an area x per unit gross area of the coal structure then the pore-air pressure acts over an area $(1 - x)$. The equivalent pore pressure will be

$$x\, U_W + (1 - x)\, U_A \tag{3.5}$$

However, as the degree of saturation decreases, the voids become mainly filled with air and the expression can be better written as

$$U_A - x\,(U_A - U_W) \quad . \tag{3.6}$$

This shows that the equivalent pressure is less than the pore-air pressure only by the pressure difference $(U_A - U_W)$ acting over an area x.

For a fully saturated material x is almost 1 so the pore pressure can be better expressed by

$$U_W = (1 - x)\,(U_A - U_W) \tag{3.7}$$

and the equivalent pressure is then approximately the pore-water pressure.

Terzaghi (1943) proposed an equation relating the total stress σ, the effective stress $\bar{\sigma}$ and the pore-water pressure U_W for saturated soils as

$$\bar{\sigma} = \sigma - U_W \quad . \tag{3.8}$$

For partially saturated coal the effective stress can be written as described by Skempton (1961).

$$\bar{\sigma} = \sigma - \left[U_A - x\,(U_A - U_W) \right] \tag{3.9}$$

For the two limits where

$$x = 1 \qquad \bar{\sigma} = \sigma - U_W \qquad \text{when } S = 1 \tag{3.10}$$

$$x = 0 \qquad \bar{\sigma} = \sigma - U_A \qquad \text{when } S = 0 \quad . \tag{3.11}$$

Since coal is initially close to saturation in insitu conditions it is more convenient to write the effective stress equation as

$$\bar{\sigma} = \sigma - \left[U_W + (1 - x)\,(U_A - U_W)\right] \tag{3.12}$$

or

$$\bar{\sigma} = \sigma - \left[1 + (1 - x)\,\frac{U_A - U_W}{U_W}\right] U_W \quad . \tag{3.13}$$

If the definition of Eq. 3.14 is made

$$R_S = 1 + (1 - x)\,\frac{U_A - U_W}{U_W} \tag{3.14}$$

then Eq. 3.13 becomes

$$\bar{\sigma} = \sigma - R_S \cdot U_W \tag{3.15}$$

If full saturation is assumed this equation reduces down to Terzaghi's equation for effective stress.

3.2.2 Capillary Tension

The drying shrinkage of coal can be attributed to several simultaneously occuring phenomena. As the natural moisture of the coal begins to evaporate from an exposed surface, a capillary tension is generated in the water which in turn introduces an effective stress increment into the material. This new effective stress increment causes a deformation in the

coal. The stresses generated at the tip of the cracks due to the capillary tension will cause the cracks to propagate as well as the formation of new cracks.

The capillary tension theory associates increased tension at the water meniscus in the capillaries with drying shrinkage. As water decreases in the capillaries, the radius of curvature increases and the surface tension forces produce a tension in the water remaining in the capillaries. This increased tension must be in equilibrium with a compressive stress in the solid. It is this compressive stress that produces the shrinkage deformation. As the drying continues the fractional amount of water decreases in the capillaries. This should cause the shrinkage strain to approach a maximum value when the moisture content of the coal is in equilibrium with the environment.

By cycling the environmental conditions a cycling of drying shrinkage can be obtained. The term hysteresis is defined as the phenomenon of changing from an initial state to a final state and back to the initial state with the paths followed on the two stages being different. Hysteresis is exhibited by the wetting and drying of coal. Experimentally it is difficult to complete more than two cycles of wetting and drying. The hysteresis of deformations in coal occurs in relation to suction potential and moisture content.

Moisture in vapor form travels through the coal in response to a suction or potential gradient. As the vapor moves

its path is obstructed and it condenses in place. This condensed moisture will reevaporate upon further drying and the cycle will continue as the moisture moves to the boundary.

3.2.3 Effective Stress

The effect of the fluid pressure in rocks is of importance in determining their time-dependent behavior. Generally, all rocks contain voids or small crack systems that may be interconnected to form channels where fluid can migrate. For most sedimentary rocks the structure is regarded as a solid skeleton traversed by a fine network of capillaries, whereas igneous rocks are considered as a solid with voids being composed of grain boundary cracks. What is necessary to describe the fluid flow in coal is a macroscopic theory for a solid containing a system of pores.

From the classical work of Terzaghi (1943) the basic effective stress law is written as

$$\sigma = \bar{\sigma} + U \tag{3.17}$$

where

σ = total stress

$\bar{\sigma}$ = effective stress

U = pore pressure

This has been described in Section 3.2.1. This relationship holds for granular soils. However, there is some disagreement on the theoretical accuracy and validity of the basic stress equation when applied to rocks.

Studies on rocks by Handin et al. (1963) and Murrell (1965) have shown that as long as rocks have connected systems of pores, the fracture and deformation is controlled by the effective stress.

Nur and Byerlee (1971) have presented perhaps the most consistent and exact solution to the calculation of effective stresses in rocks. The main assumption they made was that Hooke's Law can be used to describe the elastic strain of the material. They obtained the relationship for the stress tensor as

$$\bar{\sigma}_{ij} = \sigma_{ij} - \sigma P \delta_{ij} \tag{3.18}$$

where

$$\sigma = 1 - K/K_S \tag{3.19}$$

σ_{ij} = total stress tensor

P = confining pore pressure

δ_{ij} = Kronecker Delta

K = bulk modulus of the rock

K_S = bulk modulus of the grain

The expression does not depend directly on porosity. When the pore volume decreases to zero the pore pressure is the same as the total confining stress. From this, the strain in a porous solid with pore pressure can be determined from the elastic modulus of the solid without pore pressure if the effective stress law is used. This does not, however, take into account the time-dependent change of properties with the migration of moisture.

3.2.4 Delamination

Another process occurs simultaneously with the drying shrinkage and that is a delamination due to the presence of cracks. In the delamination, cracks parallel to the bedding planes open up at the surfaces and gradually extend inward. This enlarging of the cracks inward produces a curling of the lamina which actually expands the material in the longitudinal direction. However, a compressive axial load prevents the curling of the laminates. The delamination effect need only be considered on unloaded and drying specimens. Thus, the deformations observed on unloaded samples are the difference of contraction due to shrinkage and expansion due to delamination of the cracks.

CHAPTER 4

DRYING SHRINKAGE

4.1 Introduction

To investigate the behavior of coal due to drying shrinkage and moisture migration several series of tests were performed. These tests have been designated Series 18, 19, and 20 to correspond with the numbering of creep tests to be presented in Table 5.1. Loading-unloading tests and cyclic saturation tests are described in this chapter. Testing of elastic and strength properties related to long term testing are also presented.

4.2 Results of Test Series

Test Series 18

Series 18 was one uniaxial creep test carried out on two NX-size samples of Lincoln coal to determine the effect of loading and unloading on moist coals. The purpose of the test was to see how much strain could be recovered by removing the load after a short period of loading.

A stack of two specimens was loaded with an axial load of 500 psi. One specimen was sealed and one was unsealed. Measurement of the axial strain was then made on each specimen on the following time schedule: 0, 1/2, 1, 2, 4, 8, 16, and 24 hours.

After 24 hours, the axial load was removed and the specimens were allowed to rebound while the deformations were also measured.

The test could be run for longer periods on each part of the cycle. The reason for choosing a 24 hour period was that in practice it is during the first day after a coal seam is opened up that stability of the excavation must be obtained, and any large stress change would occur during this period. The anticipated behavior for the coal is shown in Fig. 4.1.

Fig. 4.2 shows the results of the short term loading-unloading test in Series 18. Only results for the first fifty hours are plotted so that the relevant part of the test can be seen clearly. In the first 24 hours the sealed and unsealed specimens behaved as in previous test series (to be described in detail in Chapter 6), i.e. the sealed specimen showed no time-dependent strain, while the unsealed specimen did. When the load was removed, the sealed specimen instantaneously recovered its elastic strain and the unsealed specimen recovered its elastic strain in addition to 25 percent of the time-dependent strain it had experienced during the first twenty-four hours. At this point, the sealed specimen stabilized and showed no further strain. The unsealed specimen experienced rebound for only two hours after the load was removed. During this period it recovered 1.7 percent of the total time-dependent strain it had acquired during its first twenty-four hours of testing. At twenty-six hours the unloaded, unsealed specimen began to strain again, but now at a much slower rate. The straining continued

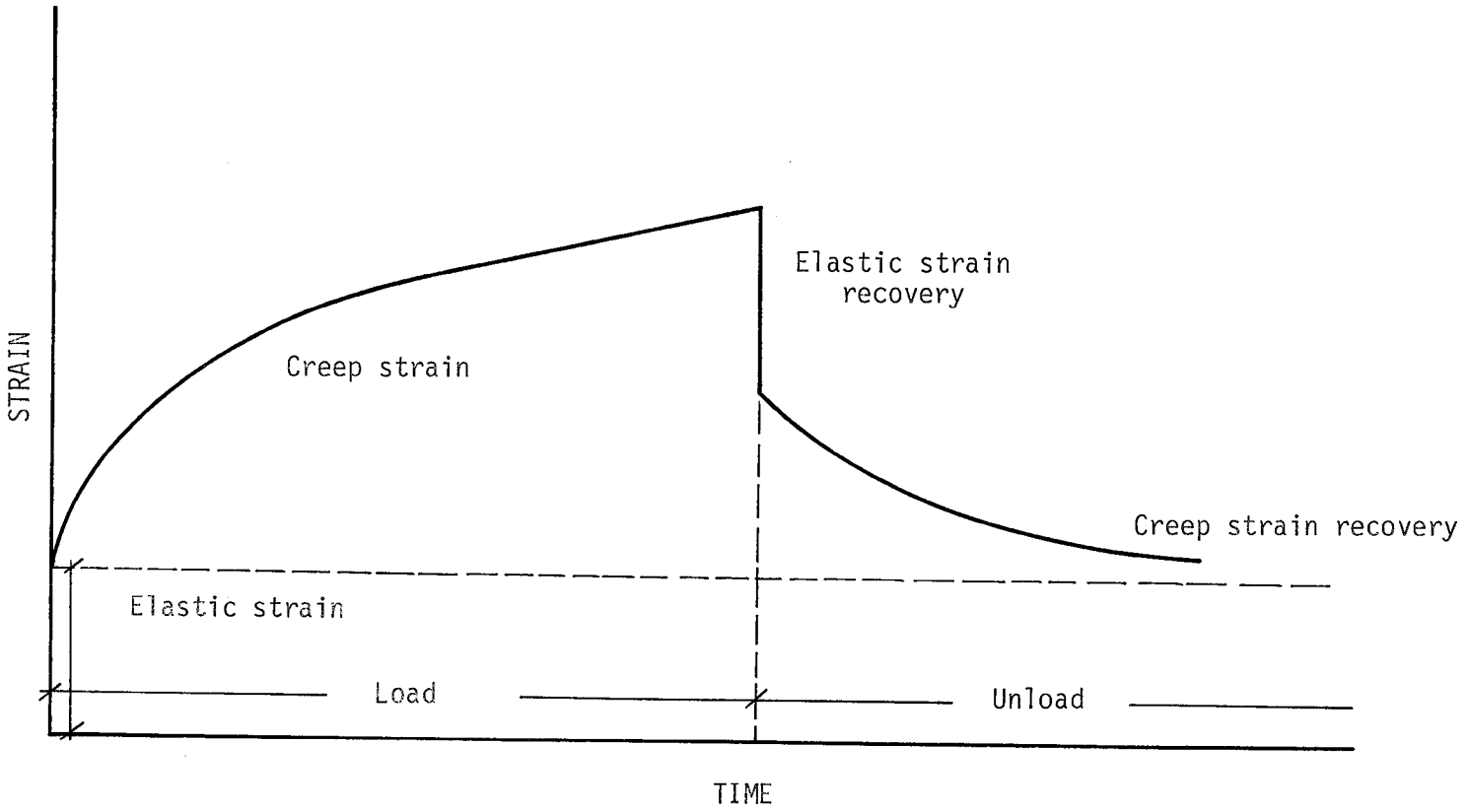

Figure 4.1 Time Dependent Creep and Recovery for a Rock Material

for one thousand hours, at which point the test was terminated. This strain was due to a continuation of the drying shrinkage without any applied external load. From twenty-four to twenty-six hours the rebound of the coal was larger than the drying shrinkage, but after twenty-six hours the drying shrinkage again became the dominant factor as shown in Fig. 4.2.

Test Series 19

Series No. 19 was run to determine the effect of cycling the water saturation on the time-dependent straining of coal in uniaxial compression. An additional part of the test was an unloading phase to get further data on the rebound of Lincoln coal.

Cyclic Saturation

It has been proposed that the creep of coal specimens under sustained load is actually due to an increase in the surface tension of the water meniscus entrapped in the coal sample. With a drying shrinkage dependency, the strain-time behavior can be related to environmental conditions. A new series of testing was proposed. The purpose was to see if all of the time-dependent strain could be recovered from an unsealed sample by immersing it in a water bath after a twenty-four hour period of drying.

Test Procedure

A standard creep testing frame as described in Chapter 2 was used to run all the tests. Since the new supply of coal from

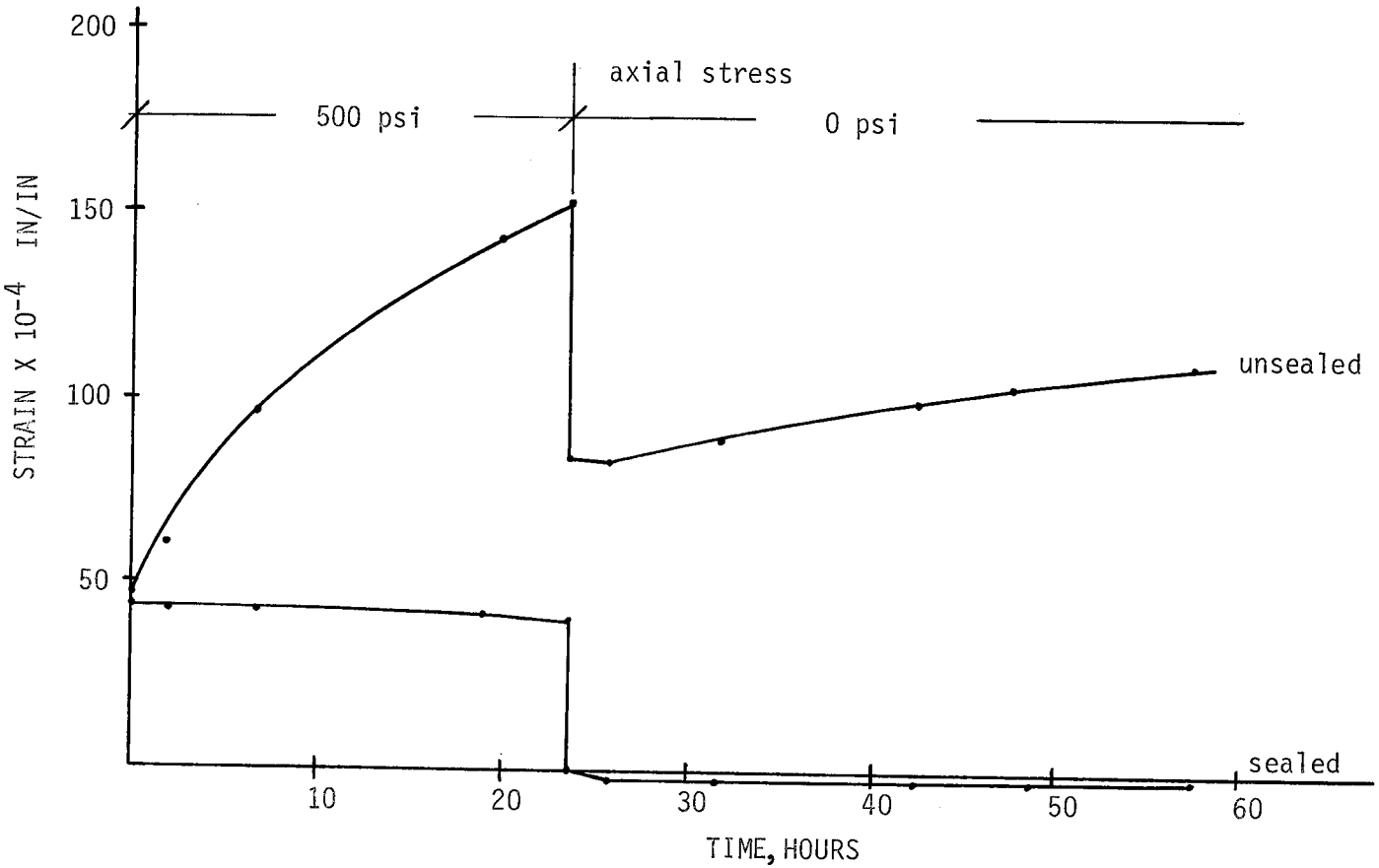

Figure 4.2 Loading-Unloading Creep of Lincoln Coal

Test Series 18

Lincoln Mine is considerably weaker under long-term loading than previous coals, lower stress levels had to be used. The testing was performed at an axial stress of 500 psi. A testing apparatus as shown in Fig. 2.5 was designed to allow a cycling of the saturation. This setup is identical to the water bath used in Series No. 16 and No. 17 (Table 5.1). The cycling of the saturation and air drying period was designed to work in the initial section of the strain-time response curve. In the first 200 hours of an uninterrupted creep test, about 80 percent of the total response of an unsealed sample occurs. Therefore, a cycle composed of twenty-four hours of wetting and twenty-four hours of drying was utilized.

Testing

Five specimens were used for this series of tests. These specimens were arranged in one stack of three that contained one sealed specimen (#1), one unsealed specimen (#3), and one cycling specimen (#2). The other two specimens (#4, #5) were set up for cycling in individual creep frames. An axial stress of 500 psi was used in all cases.

For the initial twenty-four hour period all the cycling specimens were loaded and exposed to the external environment of the testing room. Measurements of all specimens were made at 0, 0.5, 1, 2, 4, 8, 16 and 24 hours or times close to these values. After twenty-four hours the three cycling specimens were saturated. Fig. 4.3 shows the response of all five specimens during the cycle. One specimen (#4) failed after ten minutes of

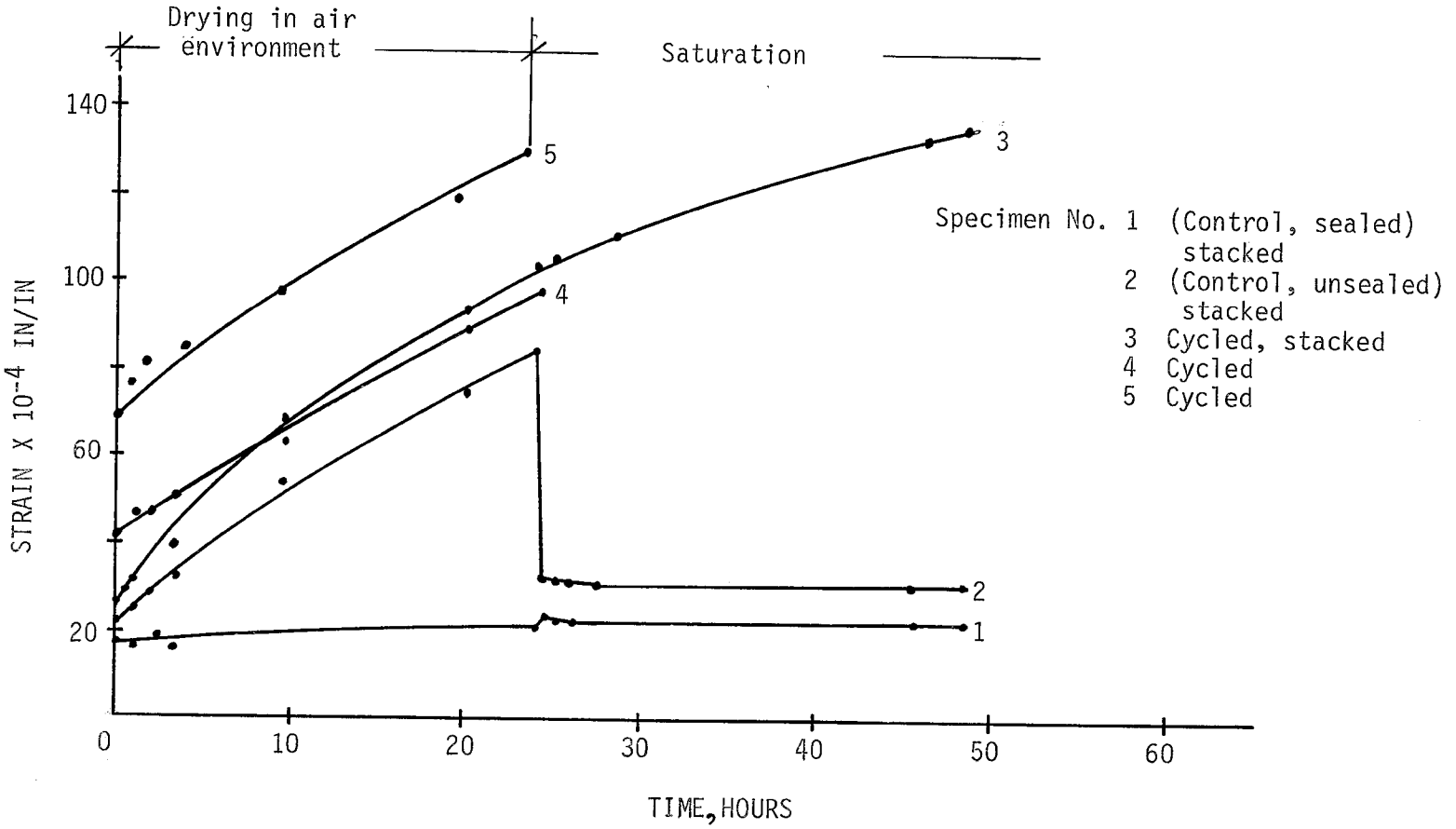

Figure 4.3 Cyclic Saturation Test on Lincoln Coal

Test Series 19 (Axial Stress = 500 psi)

saturation and the second one (#5) failed after twenty-five minutes. Disintegration of the specimens can be attributed to the water entering the newly formed cracks and creating a negative pore pressure. According to the postulate of effective stress principle as propounded in Chapter 3, this pore pressure caused an effective compressive stress increment to develop, which in turn dislodged small pieces from the surface of the specimen. Rapid and total failure soon followed. The third cycling specimen (#2) remained somewhat intact. Total failure did not occur, but the specimen experienced progressive deterioration. This specimen that remained intact experienced substantial rebound in the first half hour after saturation. During the following twenty-four hours of saturation it showed only a very small continuation of the rebound. The specimen recovered 86 percent of its time-dependent strain after being saturated for twenty-four hours.

Test Series 20

Test Series 20 was performed as a continuation of Series 19 to obtain the response of coal to cyclic saturation. Four unsealed specimens were set up separately in individual standard creep frames and allowed to strain for twenty four hours at 500 psi. The specimens were then saturated in water baths and allowed to rebound. Upon saturation, one of the specimens (#4) failed after a short period of time as shown in Fig. 4.4. The testing continued for one and one-half cycles of drying and saturating on the three remaining specimens. Fig. 4.4. shows

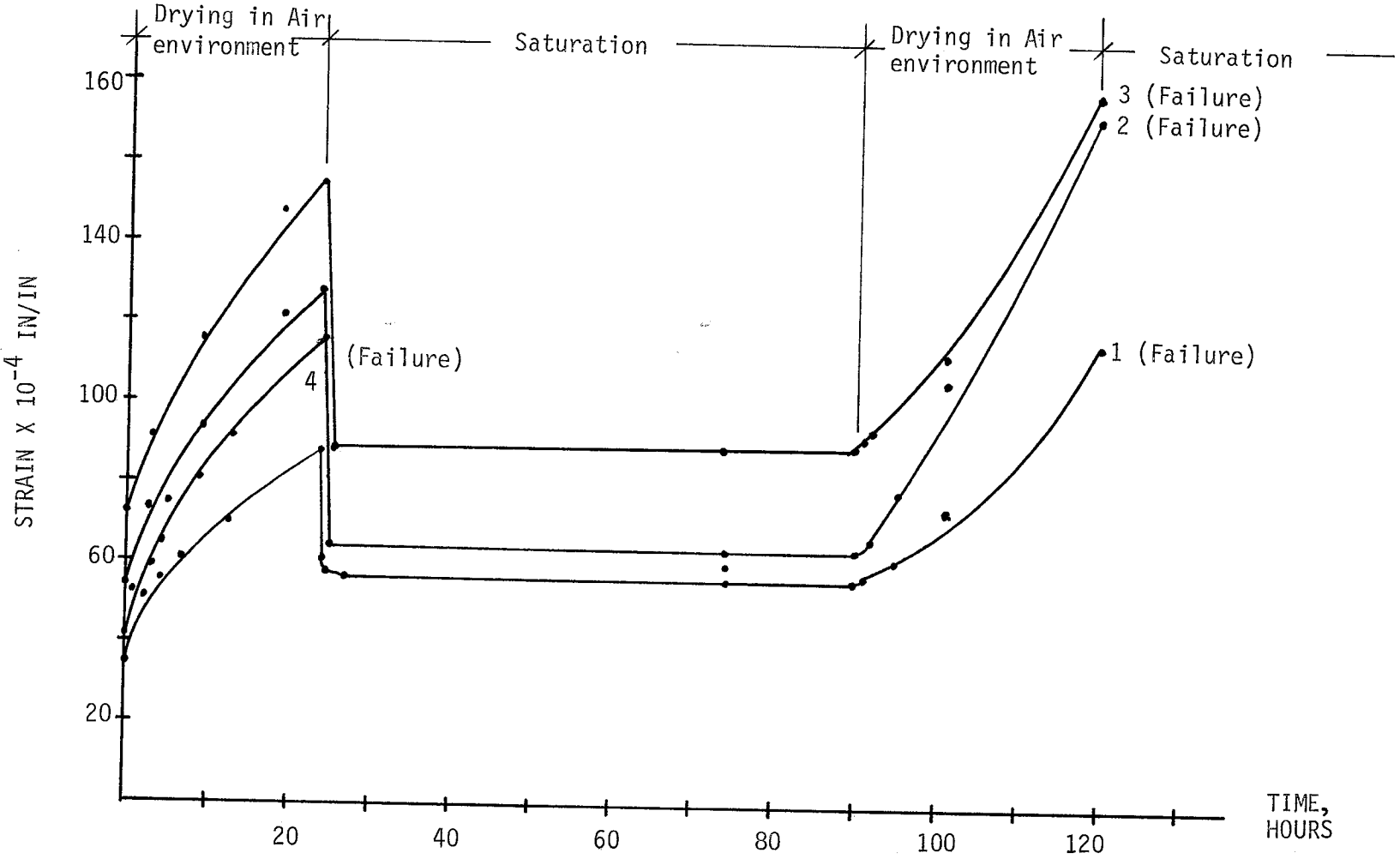

Figure 4.4 Cyclic Saturation Test on Lincoln Coal
Test Series 20 (Axial Stress = 500 psi)

the results of one and one-half cycles of the test. Upon the saturation of the specimens the second time they all failed after short periods of time.

Similar results were obtained corresponding to Series 19. The three specimens that remained intact (#1, #2, #3) through one and one-half cycles rebounded, with the rebounds shown in Table 4.1.

TABLE 4.1

REBOUND OF SAMPLES
DUE TO SATURATION

Specimen #	Ultimate rebound of creep strain
2	61%
3	87%
4	78%

From the data collected in this series, the following comments can be offered. By exposing coal under uniaxial compression to a continuous cycling of drying and wetting, a cycling of axial strain is obtained. During the initial drying cycle the coal behaves as in previous creep tests with increasing strain at a decreasing strain rate. When the specimens are subjected to saturation again, a rebound or recovery of the time-dependent strain occurs. This recovery has been found to be from 60 percent to 90 percent of the time-dependent strain. The ultimate amount of strain recovery occurs within three hours

after saturation. Once the ultimate recovery is reached, there is no further strain until the saturation is removed.

On the second cycle of drying the strain rate is higher than during the first drying period. This is due to a progressive deterioration of the coal material with a growth of cracks and formation of new cracks. Cracking is visible throughout the specimens.

Upon saturating the specimens a second time, total failure occurs. The samples have deteriorated to a point where the structure is so weak it cannot withstand any increase in effective stress caused by a negative pore water pressure from the saturation process. At this point the coal fractures into many pieces due to the large network of cracks.

Testing of Elastic and Strength Properties Related to Long-term Testing

Only a brief discussion of the elastic properties of coal is presented, since Sture (1976) and Martin (1972) have provided comprehensive works on the subject. The elastic strain produced on coal is proportional to the stress applied through the Young's Modulus. The elastic strain is instantaneous upon the application of stress and is recovered instantaneously after the stress is removed. When coal is under a sustained load, the Young's Modulus of the material decreases somewhat over a period of time. Correspondingly, the elastic strain will increase somewhat. This is shown in Fig. 6.2.

Post Creep Testing Strength and Elastic Tests

After 4,500 hours of sustained uniaxial loading of Paonia coal (test Series 15, see Table 5.1) followed by 1,500 hours of rebound under zero load, these specimens were tested for elastic stress-strain properties and uniaxial strengths. Table 4.2 shows the unconfined compressive strength (q_u) obtained by loading the specimens to failure. The sealed specimens were assumed to behave as intact coal since no strain occurred during long term testing.

TABLE 4.2

RESULTS OF UNIAXIAL STRENGTH TESTS

Sealed Specimens		Unsealed Specimens	
Previous sustained uniaxial stress	Uniaxial strength	Previous sustained uniaxial stress	Uniaxial strength
psi	psi	psi	psi
250	3,140	250	2,281
500	2,039	500	1,140
750	3,042	750	3,169
1,000	2,423	1,000	1,690
Avg. q_u wet = 2,661 psi		Avg. q_u dry = 2,070 psi	
Std. Dev. = 800 psi		Std. Dev. = 868 psi	

This test gave a ratio of q_u wet/q_u dry of 1.28.

The results of the eight elastic stress-strain experiments on NX-size specimens can also be used to compare the

Young's Modulus of the sealed specimens to that of the unsealed. The ratio of wet to dry Young's Modulus for coal was found to be 1.26. This value is quite different from those given by Wiid (1970) for other types of rock, as shown in Table 4.3.

TABLE 4.3

COMPARISON OF WET VERSUS DRY YOUNG'S MODULI FOR CERTAIN ROCKS, WILD (1970)

Rock Type	Young's Modulus Wet/Dry
Dolerite	.97
Sandstone	.7 - .84
Silty Shale	.43
Arenaceous Shale	.7

In most rock types water saturation tends to decrease stiffness by creating lubricated surfaces within the rock structure that slide more easily. However, in coal a different process prevails which creates shrinkage cracks upon the loss of moisture, when initially the moisture holds all of the micro-cracks closed and strengthens the material. A loss of moisture causes a decreased stiffness due to the many cracks that have formed. This helps support the theories presented previously.

A comparison of the ratio of Young's Modulus for wet and dry specimens of different coals further supports the theories presented. In Table 4.4 the results of several elastic stress-strain tests are presented for Lincoln and Paonia coal. The

relative values of Young's Modulus are quite different. This can be explained by the larger amount of moisture loss in Lincoln Coal.

TABLE 4.4

MOISTURE CONTENT AND YOUNG'S MODULUS FOR TWO COALS

Coal Type	Moisture Content (%)	Young's Modulus Wet/Dry
Paonia	11	1.26
Lincoln	34	1.56

4.3 Conclusions

From the loading-unloading test on Lincoln coal, the following conclusions can be made:

1. The instantaneous elastic strain is recovered immediately after the load is removed from the specimen.

2. There is a time-dependent rebound of coal. This would probably be more dramatic if the test was run on a 48-hour cycle.

3. After twenty-four hours there is still moisture migration causing the straining of unloaded Lincoln coal.

4. If the coal was allowed to dry and deform for a longer period of time, the rebound would have a larger magnitude than the continuing shrinkage strain and a greater time-dependent strain recovery would be seen.

From the cyclic drying and wetting test on Lincoln coal, the following conclusions may be drawn:

1. The creep strains of Lincoln coal are quite significant, being comparable to the strains of other moist coals, and should be considered in engineering calculations for the time-dependent deformations.

2. By testing specimens in a water bath, the formation of menisci could not take place even though moisture migration was allowed. The absence of the time-dependent strains indicates that such strains are not induced by moisture migration, ruling out the process of consolidation as the prime cause of such strains.

3. By testing specimens exposed to a dry environment, the escape of moisture allowed the formation of menisci. This leads to the creation of negative pore water pressure in the cracks, which in turn leads to an effective compressive stress increment. Such process is responsible for the time-dependent strains observed in coal.

From the testing of elastic and strength properties related to long term testing, it can be concluded that coal behaves differently than most rock types. Also, moisture migration causes a decrease in the strength and elasticity of coal, whereas most rock types increase in strength and elasticity with a loss of moisture. In addition, the decrease in elasticity is higher for wetter coals than for dryer coals.

CHAPTER 5

UNIAXIAL CREEP TESTS

5.1 Introduction

With the results of testing of the creep response of coal at the University of Colorado, a good base of test data has been obtained. Over this period 240 samples have been tested from six different mines.

Table 5.1 gives a summary of all the creep testing done on Eagle, Gillette, Paonia, and Lincoln coal. Testing of Federal #1 and York Canyon coal was very limited and since the creep observed was almost negligible none of those testing results are presented here.

Table 5.2 shows some of the fundamental mechanical and chemical properties of the six coal types tested (U.S. Coal Mine, 1976; Pilmore, 1969).

This chapter is a review of all of the work that has been accomplished on creep strain during the Bureau of Mines sponsored project, "Constitutive Relations of Coal and Coal Measure Rocks". The results of test Series 1 through 17 are reported here. Series 18 through 20 were discussed in Chapter 4.

TABLE 5.1

SUMMARY OF UNIAXIAL CREEP AND SHRINKAGE TESTING PERFORMED

Series No.	Coal Type	Humidity %	No. of Spec.	Stress Level psi	Start	End	Total Time, hrs.	Purpose	Reference
1	Gillette $\alpha=0$	52	2	0	2/11/74	2/13/74	51	Effect of Specimen Orientation, Gillette Coal	Ko and Gerstle, 1974
			4	250					
	Gillette $\beta=0$	52	2	0	1/28/74	2/18/74	506		
			4	250					
	Gillette $\gamma=0$	52	2	0	1/23/74	4/22/74	2,110		
			4	250					
2	Eagle $\alpha=0$	52	2	0	3/11/74	4/9/74	654	Effect of Specimen Orientation, Eagle Coal	Ko and Gerstle, 1974
			4	300					
	Eagle $\beta=0$	52	2	0	3/13/74	4/23/74	991		
			4	250					
	Eagle $\gamma=0$	50	2	0	3/6/74	4/22/74	1,130		
			4	250					
		50	2	0	4/15/74	5/22/74	883		
			4	250					

TABLE 5.1 (continued)

SUMMARY OF UNIAXIAL CREEP AND SHRINKAGE TESTING PERFORMED

Series No.	Coal Type	Humidity %	No. of Spec.	Stress Level psi	Start	End	Total Time, Hrs.	Purpose	Reference
3	Eagle γ=0	50	2	0	4/25/74	6/7/74	1,030	Load and	Ko and
			4	250				Humidity	Gerstle,
			4	500	4/25/74	5/23/74	666	History,	1974
			4	750				Eagle Coal	
4	Eagle γ=0	50	2	0	4/24/74	10/28/74	3,769	Effect of	Ko and
			4	400		11/1/74	3,873	Stress	Gerstle,
			4	650		7/13/74	1,035	Level,	1974
			4	1,000		8/30/74	2,323	Eagle Coal	
5	Eagle γ=0	50	2	0	6/12/74	11/1/74	3,237	Effect of	Ko and
			4	500		7/10/74	675	Stress	Gerstle,
			4	750		6/17/74	121	Level,	1974
								Eagle Coal	

TABLE 5.1 (continued)

SUMMARY OF UNIAXIAL CREEP AND SHRINKAGE TESTING PERFORMED

Series No.	Coal Type	Humidity %	No. of Spec.	Stress Level psi	Start	End	Total Time, Hrs.	Purpose	Reference
			4	1,000		11/1/74	3,237	(Eagle Coal)	
			4	1,250		6/28/74	389		
6	Gillette γ=0	52	2	0	7/13/74	9/19/74	1,619	Effect of	Ko and
			4	200			1,619	Stress	Gerstle,
			4	300	7/17/74	8/14/74	671	Level,	1974
			4	400	7/13/74	8/12/74	694	Eagle Coal	
			4	500	7/17/74	8/8/74	517		
			4	600	7/13/74		629		
7	Gillette γ=0	56	3	0	8/22/74	10/7/74	1,129	Effect of	Ko and
			4	200	8/21/74	10/9/74	1,171	Humidity,	Gerstle,
			4	400	8/22/74	9/19/74	708	Gillette	1974
		20-55	3	0			708	Coal	

TABLE 5.1 (continued)

SUMMARY OF UNIAXIAL CREEP AND SHRINKAGE TESTING PERFORMED

Series No.	Coal Type	Humidity %	No. of Spec.	Stress Level psi	Start	End	Total Time, Hrs.	Purpose	Reference
			4	200		9/11/74	486	(Gillette	
			4	400		9/26/74	94	Coal)	
8	Eagle γ=0	50-64	1	0	12/7/74	5/2/75	3,533	Effect of	Ko and
			2	250			3,533	Humidity on	Gerstle,
			2	500			3,523	Eagle Coal	1976
			2	750			3,514		
		12-16	1	0	12/8/74	1/9/75	760		
			2	250		5/2/75	3,573		
			2	500		1/13/75	864		
			2	750		12/19/74	261		
9	Eagle γ=0	20	1	0	5/8/75	6/23/75	1,272	Effect of	Ko and
			2	250		7/22/75	1,798	Humidity on	Gerstle,

TABLE 5.1 (continued)

SUMMARY OF UNIAXIAL CREEP AND SHRINKAGE TESTING PERFORMED

Series No.	Coal Type	Humidity %	No. of Spec.	Stress Level psi	Start	End	Total Time, Hrs.	Purpose	Reference
			2	500		6/3/75	450	Eagle Coal	1976
			2	750		7/22/75	1,798		
		55	1	0		5/30/75	528		
			2	250		7/22/75	1,798		
			2	500		7/22/75	1,798		
			2	750		7/22/75	1,798		
		95	1	0		7/8/75	1,428		
			2	250		7/9/75	1,452		
			2	500		7/9/75	1,452		
			2	750		7/9/75	1,452		
10	Eagle γ=0	50	2	0	7/23/75	10/27/75	2,304	To obtain	Ko and
			3	150		5/9/76	6,916	data at	Gerstle,
			3	300		5/9/76	6,916	additional	1976

TABLE 5.1 (continued)

SUMMARY OF UNIAXIAL CREEP AND SHRINKAGE TESTING PERFORMED

Series No.	Coal Type	Humidity %	No. of Spec.	Stress Level psi	Start	End	Total Time, hrs.	Purpose	Reference
			3	450		5/9/76	6,916	stress	
			3	600		12/20/75	3,566	levels for	
			2	750		5/9/76	6,916	Eagle Coal	
11	Big Horn γ=0	50	2	0	3/19/76	6/22/76	3,800	Effect of	Ko and
			2	150				stress on	Gerstle,
			2	300				Big Horn	1977
			2	450				coal. Rela-	
			2	600				tion lateral	
			2	750				& axial	
								strain	

TABLE 5.1 (continued)

SUMMARY OF UNIAXIAL CREEP AND SHRINKAGE TESTING PERFORMED

Series No.	Coal Type	Humidity %	No. of Spec.	Stress Level psi	Start	End	Total Time Hrs.	Purpose	Reference
12	Big Horn γ=0	50	5	1,000 increased stepwise to failure Max. 2,500	8/13/76	12/13/76	3,600	To find threshold stress level at which creep will occur in Big Horn coal	Ko and Gerstle, 1977
13	Eagle γ=0	50	5	1,000	8/30/76	11/14/76	1,850	To find threshold stress level at which creep will occur in Eagle coal	Ko and Gerstle, 1977

TABLE 5.1 (continued)

SUMMARY OF UNIAXIAL CREEP AND SHRINKAGE TESTING PERFORMED

Series No.	Coal Type	Humidity %	No. of Spec.	Stress Level psi	Start	End	Total Time Hrs.	Purpose	Reference
14	Big Horn γ=0 Hollow core		1	Hollow core 400 psi (vac)	10/18/76	12/17/76	1,400	To check moisture drainage with a hollow core sample	Ko and Gerstle, 1977
			1	Hollow core 600 psi (vac)					
			1	Hollow core sealed outside 400 psi (vac) 50 psi (conf)					
			1	Hollow core sealed 600 psi (vac) 50 psi (conf)					
			1	solid sealed w/wax 400 psi					
			1	solid sealed w/wax 600 psi					

TABLE 5.1 (continued)

SUMMARY OF UNIAXIAL CREEP AND SHRINKAGE TESTING PERFORMED

Series No.	Coal Type	Humidity %	No. of Spec.	Stress Level psi	Start	End	Total Time Hrs.	Purpose	Reference
15	Paonia γ=0	50	2	250	11/3/77	7/17/78	5,450	Effect of stress on Paonia coal. Effect of unloading on rebound of coal	
			2	500					
			2	750					
			2	1,000					
			2	0 (Weight Control)					
16	Lincoln γ=0	50	2	0	4/20/78	4/24/78	100	Alternate method of sealing specimen. Effect of stress on Lincoln coal.	
			2	1,000					

TABLE 5.2

MECHANICAL AND CHEMICAL PROPERTIES OF COALS TESTED

Mine Location	Classification	Range of Moisture %	Vol. Matter %	Fixed Carbon %	Ash %	Sulphur %	B.T.U.	E psi	q_u psi
Big Horn Gillette, Wyo.	Subbituminous B	22.8-34.7	42.2	51.9	5.7	0.6	12,300	N.A.	1,500
Eagle Erie, Colo.	Subbituminous B	15.5-34.1	39.7	51.5	8.4	0.6	9,860	4×10^5	2,100
Bruceton Bruceton, Pennsylvania	High-Volatile B Bituminous	1.5-3.2	36.7	54.5	8.7	1.6	13,640	5×10^5	N.A.
Lincoln Erie, Colo.	Subbituminous B	15.5-34.1	39.7	51.5	8.4	0.6	9,860	4×10^5	2,100
Orchard Valley, Paonia,Colo.	High-Volatile C Bituminous	6.0-11.6	40.2	53.5	8.9	0.9	13,500	5×10^5	2,400
York Canyon Raton, New Mexico	High-Volatile B Bituminous	1.0-3.8	35.7	54.9	8.8	0.6	14,340	3×10^5	N.A.

5.2 Results of Test Series

Test Series 1 and 2

Since coal is an anisotropic medium, with preferred orientations defined by the normals to the major cleat, minor cleat, and bedding planes (designated by $\alpha=0$, $\beta=0$, and $\gamma=0$, respectively) it might be expected that the direction of the uniaxial stress application affects the creep of the material. To check on this variable, Series 1 and 2 were performed at similar stress levels and under identical environmental conditions on specimens of Gillette and Eagle cored in the three principal material directions.

It was readily seen that the scatter of the creep strain of two identical samples is in general larger than the difference in strains of specimens of different orientations for each material. It appeared that specimen orientation is a minor factor and henceforth this parameter was neglected. All further creep specimens were cored with their axes normal to the bedding plane, that is, $\gamma=0$, since it was deemed that the overburden stress might be the chief cause of creep in coal mine openings and pillars.

It was also apparent that the creep in the moister Gillette coal was considerably larger than that of Eagle coal.

Test Series 3, 4, and 5

The creep curves of Figs. 5.1, 5.2 and 5.3 for Eagle coal were compiled from the results of test Series 3, 4, and 5.

The various parameters which influenced the creep are discussed below.

The applied uniaxial stress should be related to the short-time material strength. There was a great variation of this short-term strength; values range from a minimum of 850 psi to a maximum of 3,300 psi, for an average strength of 2,080 psi. The highest sustained load on an Eagle creep specimen was 1,250 psi for a time of 280 hours to failure. It was clear that a certain randomness was to be expected in the ability of this coal to sustain such high load levels.

Fig. 5.1 shows plots of total strain versus time for different stress levels ranging from σ=0 for the control cylinders to a maximum of σ=1,250 psi. A minimum of two unsealed specimens within each stack was available; for some stress levels, more than one stack was tested. In all cases, all available creep curves from tests within the controlled environment room were averaged to obtain the summary curves of Fig. 5.1.

It is seen that in general the average total strain increases with stress level. For a low stress of 250 psi, the creep strain is but slightly larger than that for the unloaded control specimen. Greater creep strain is observed for 400 psi, but only slight further increase of strain results from higher loads.

The independence of the creep strain of the stress above the threshold level of 400 psi is further emphasized by subtracting the instantaneous strain. Fig. 5.2 shows the time-dependent

portion of the total strains up to 300 hours of sustained loading. The creep curves for stress levels from 400 psi to 1,250 psi practically coincide.

For those stress levels for which strains were obtained for long loading times, that is, 400 psi and 1,000 psi, a constant strain rate regime appears in Fig. 5.1 beyond 1,000 hours. This steady-state creep amounts to about 3.5×10^{-3} in/in per 1,000 hours at 400 psi, and 7.0×10^{-3} in/in per 1,000 hours at 1,000 psi. Further long-time creep tests are necessary to verify the existence of such a steady-state creep regime for all stress levels. It is interesting to observe this continuing creep long after the control specimens have stabilized at their final dimensions.

The series consisted of stacks of two unsealed specimens, and two sealed by a wax coating against moisture loss. None of the sealed specimens showed any creep. After a period of about 20 days, the wax was stripped from the sealed specimens, and subsequent creep was observed. Fig. 5.3 compares the behavior of the originally and newly unsealed specimens at two different stress levels up to a time of 2,000 hours. It is observed that after a sufficient period of time, the strain in the initially sealed specimens tends to catch up with that in the unsealed specimens when the internal moisture condition attains equilibrium with the environmental humidity.

All results presented so far were obtained at one set of environmental conditions of about 52 percent relative humidity

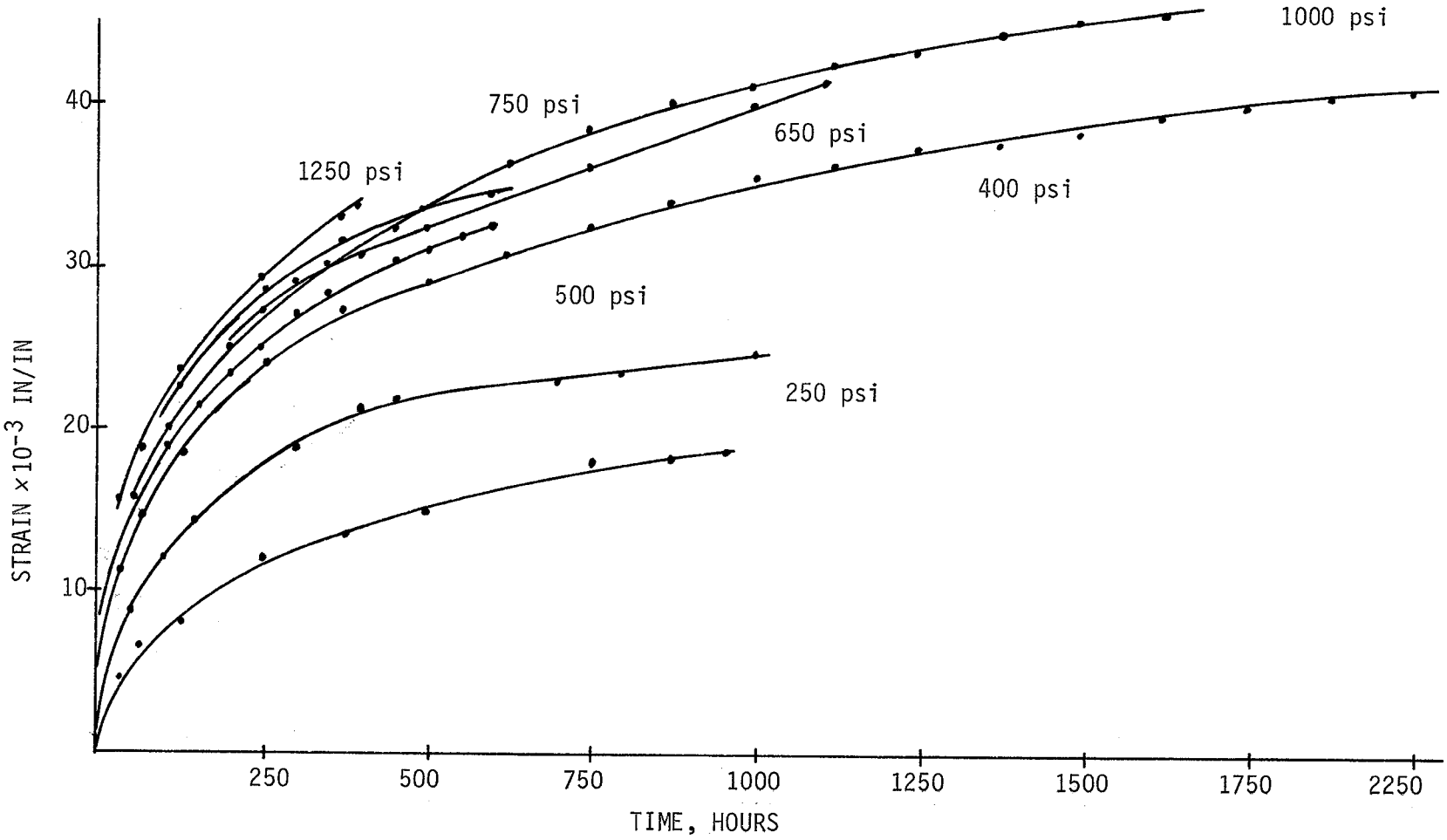

Figure 5.1 Effect of Stress Level on Creep of Eagle Coal Test Series 3, 4 and 5.

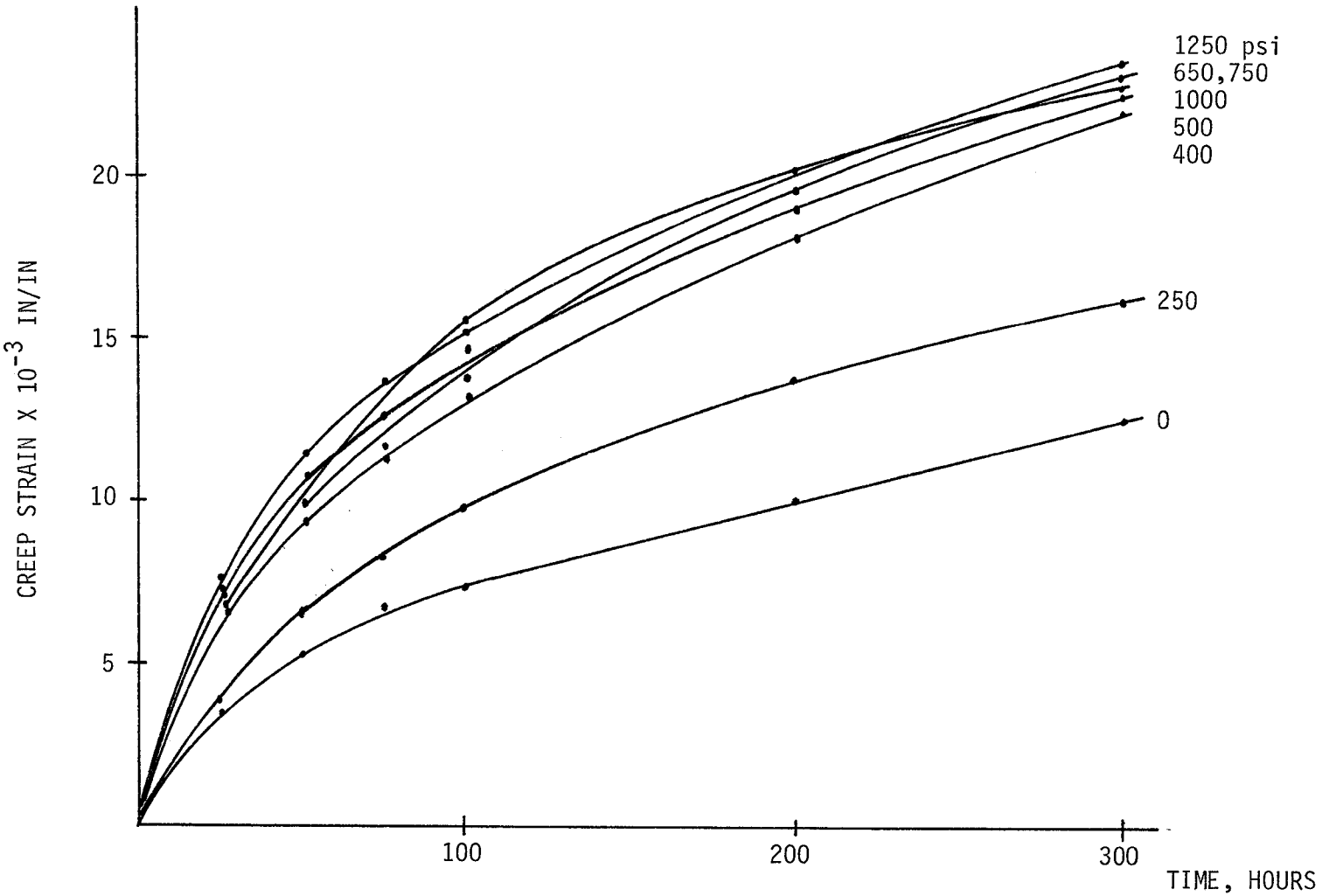

Figure 5.2 Creep Strain of Eagle Coal Test Series 3, 4 and 5.

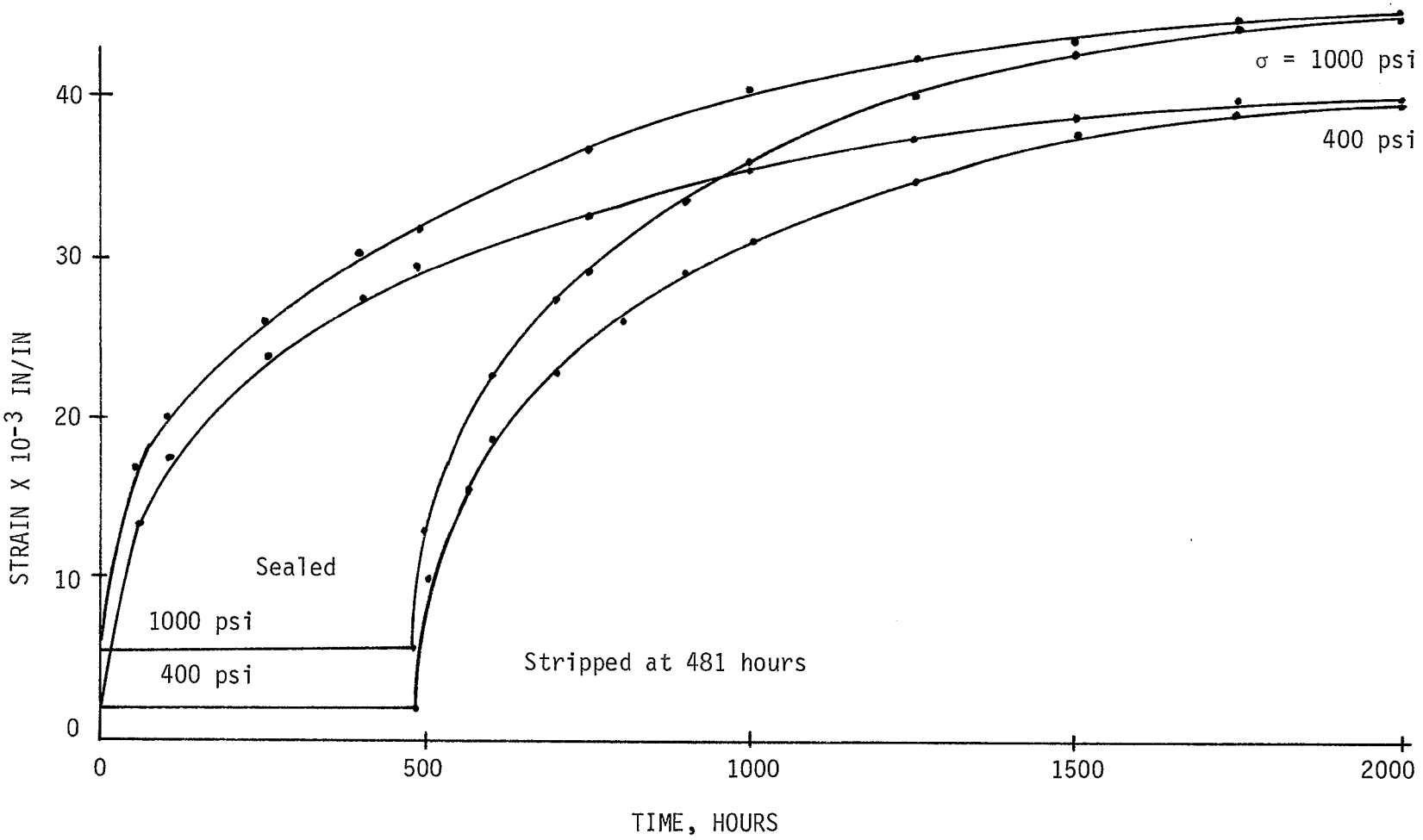

Figure 5.3 Effect of Moisture History on Creep of Eagle Coal Test Series 5

and 80°F temperature. The observations of the preceding sections regarding moisture migration imply that the ambient humidity may be a major parameter affecting creep. Analysis of this moisture dependency was performed in test Series 8.

Test Series 6 and 7

Coal from the Wyodak Open-Pit Mine in Gillette, Wyoming, was selected for testing as an example of a high-moisture western coal. This material shows great variability in its properties, as in the uniaxial short-time strength results. The specimens of this coal showed more fissures than Eagle coal, and all results indicated correspondingly greater random scatter.

Fig. 5.4 shows the creep behavior at all stress levels up to a time of about 15 days; all curves represent the average of two specimens, kept under similar environmental conditions of about 50 to 55 percent humidity, and a temperature of 80 to 80°F. The recorded behavior is highly erratic; while all curves show the same general trend, no cause and effect relationship is apparent between stress level and creep.

A further puzzling fact is that whereas the moisture loss of the control cylinder of Series 6 shows much greater moisture loss than that of Series 7, yet the dimensional changes are much greater for the latter. This seems in conflict with the earlier hypothesis which associates a major portion of creep at early age with moisture loss, and no explanation can be offered for this observation.

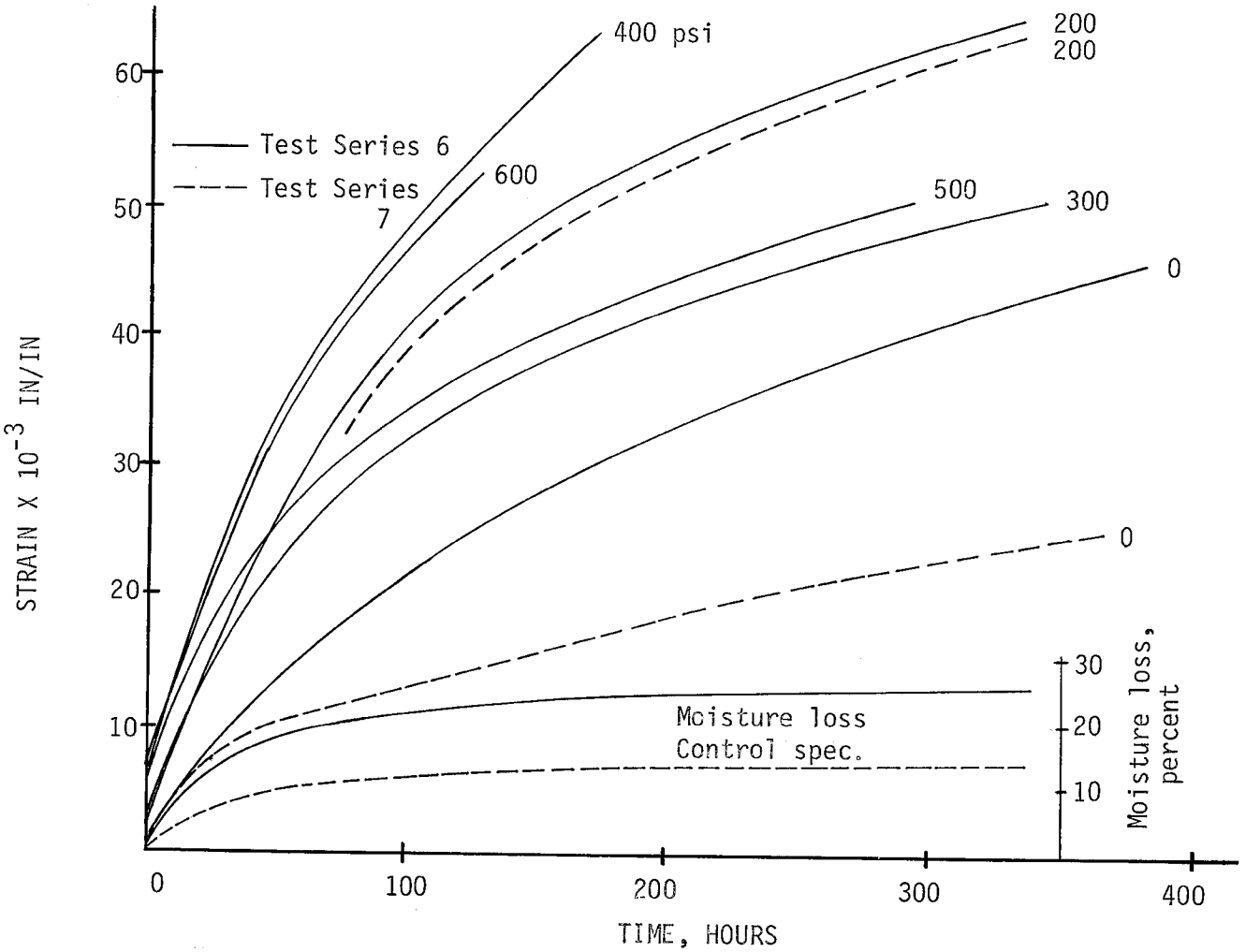

Figure 5.4 Effect of Stress Level on the Creep of Gillette Coal Test Series 6 and 7.

Strains in the loaded specimens of this coal attained such high values, in excess of 60 x 10^{-3} in/in, that they exceeded the capacity of the available strain measuring instrumentation. For this reason most of these tests had to be discontinued prior to any attainment of a steady-state regime.

It must be concluded from these results that the random material variation from one specimen of Gillette coal to the next overshadows any functional relationships between stress and creep strain. It follows that a systematic investigation must be based on a probabilistic approach which requires a large number of replications of these tests for a sound statistical basis. The expenditure of time and effort required for this appears quite exorbitant.

To detect the effects of ambient humidity on the creep of Gillette coal, Series 7 compared the behavior of stacks of specimens under 200 and 400 psi stress at two different locations, one in the environment room (whose controls were inoperative at the time, as discussed earlier) at humidities ranging from 50 to 64 percent, the other exposed to the outside climate, with humidities from 20 to 55 percent. Because of these erratic conditions, no clear cut results could be obtained. Oddly enough, creep at higher humidity levels was more pronounced. Whether this is due to random variation of the material or due to unexplained systematic effects is not known.

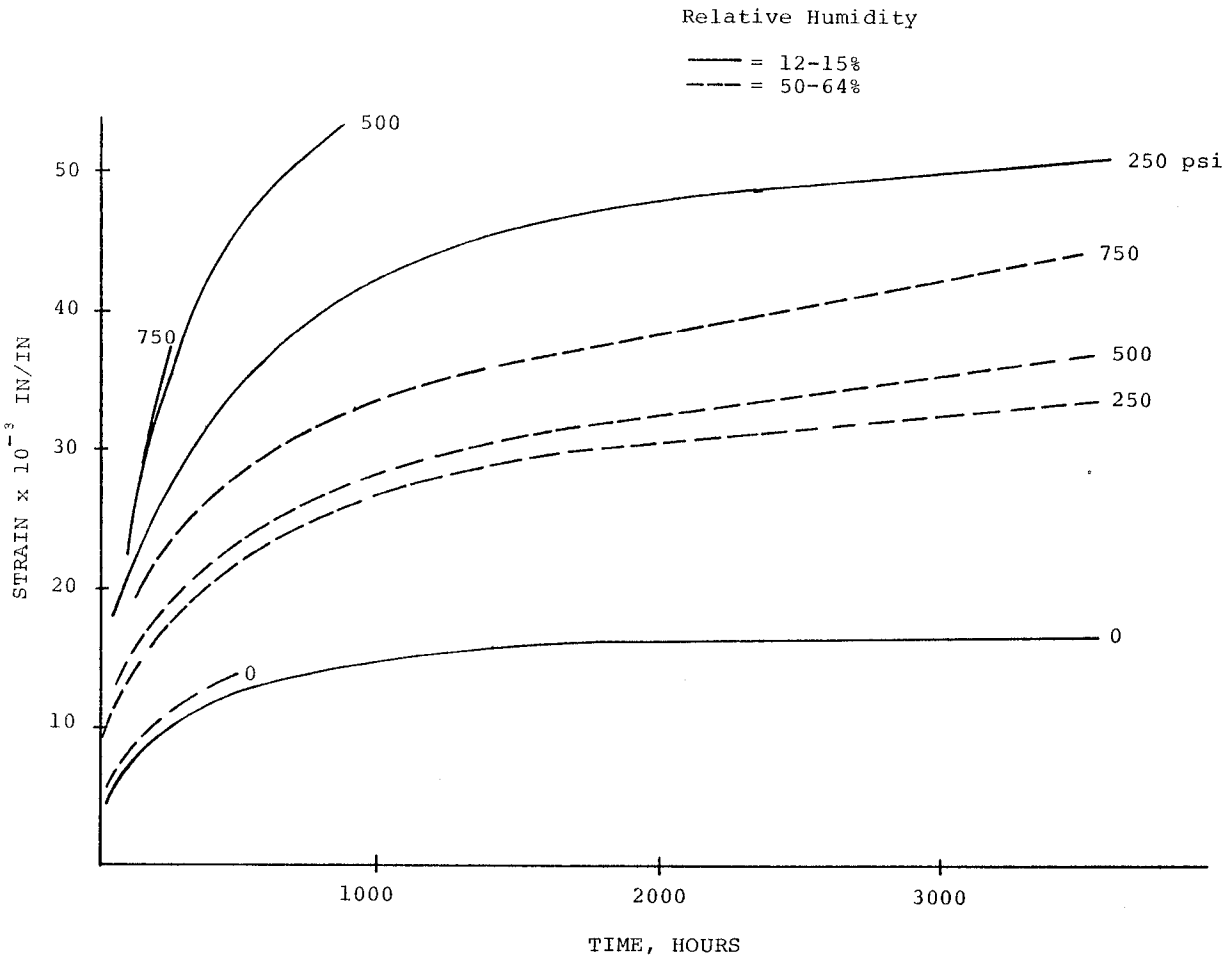

Figure 5.5 Creep Strain Curves of Eagle Coal at Various Humidity Levels Test Series 8

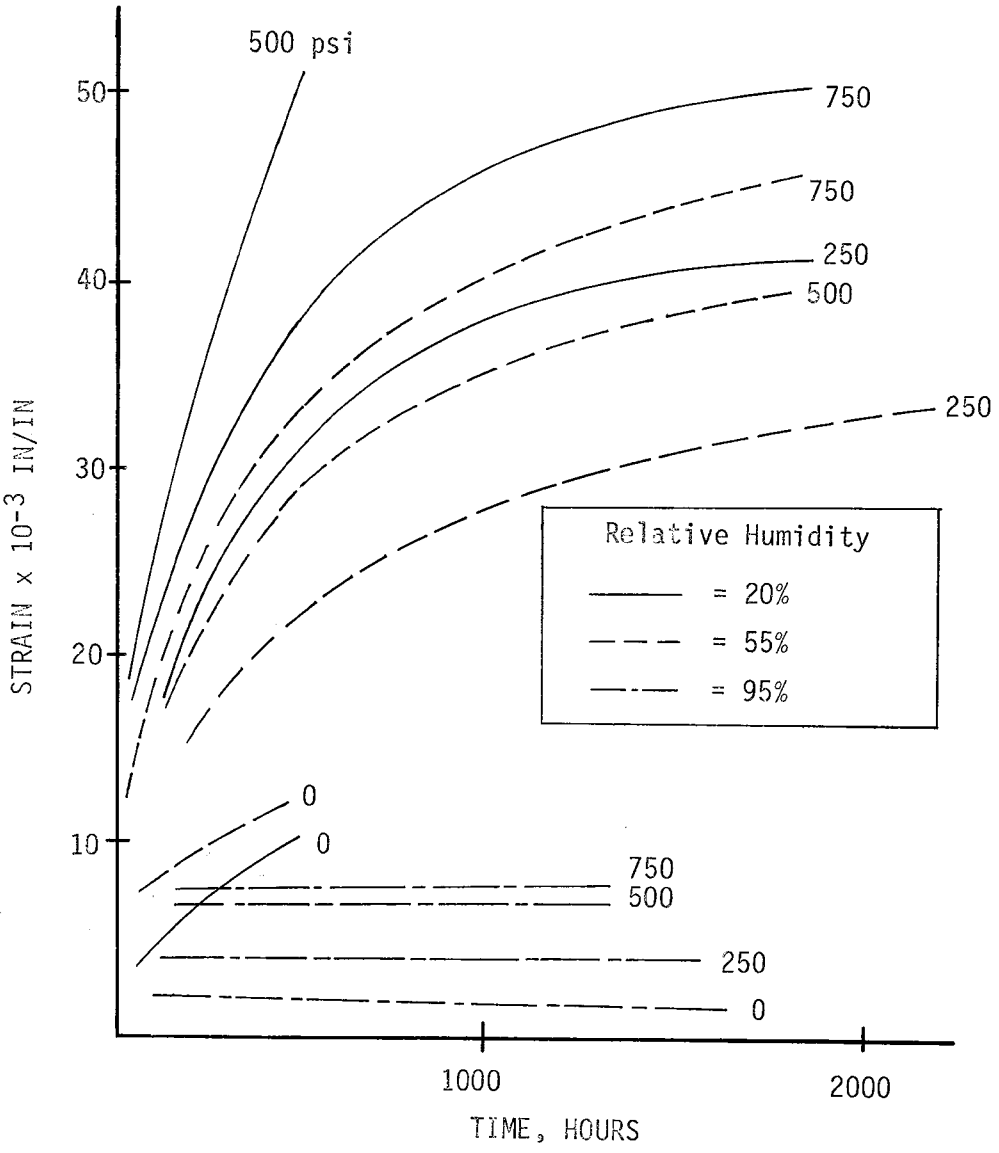

Figure 5.6 Creep Strain Curves for Eagle Coal at Various Humidity Levels

Test Series 9

were of nominally identical material, but procured at different times, and tested under supposedly identical conditions, indicate that prediction of coal behavior will at best be possible on a probabilistic basis.

Test Series 10

Series 10, designed to complement the stress levels tested in Series 8, was to provide additional data on the effect of stress with respect to time. Other factors contributing to creep were held constant with standard conditions set at 50-55% humidity and 70-75^{o}F temperature. Series 10 was designed with applied stresses nested in the stress levels of Series No. 8, so as to complement the earlier data.

The strain vs. time results of Series 10 are shown in Fig. 5.7. The general trend here confirms earlier results which show that creep tends to attain a constant magnitude with increasing stress levels.

Test Series 11

Series 11 was a set of uniaxial creep tests carried out on Big Horn coal. Axial and lateral strains were recorded, but only the axial strain measurements are analyzed here.

Fig. 5.8 shows the average values of axial and lateral strain obtained from two specimens at each stress level for the entire test period. As observed before on Eagle coal, a constant strain rate regime appears beyond 2,000 hours under sustained load;

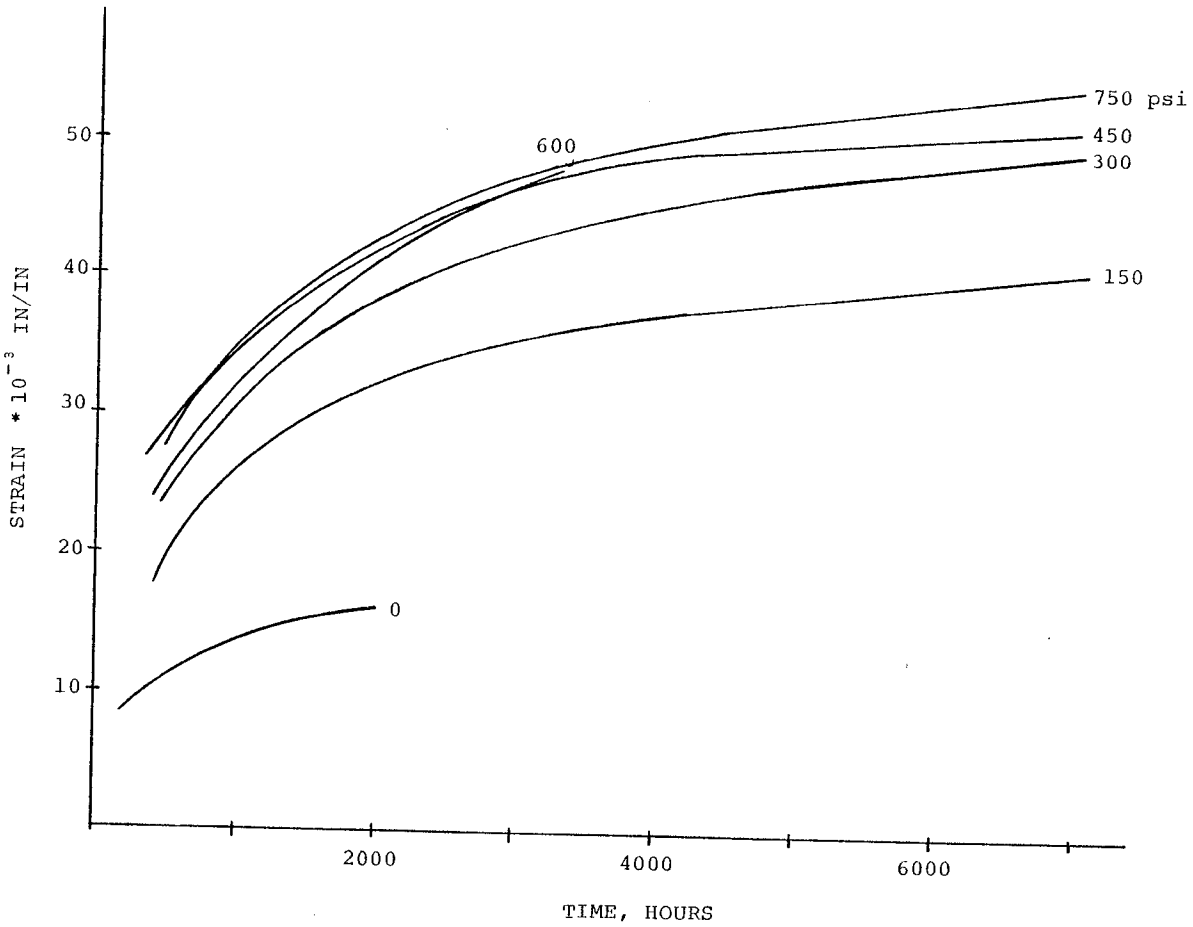

Figure 5.7 Creep Strain Curves for Eagle Coal Test Series 10

for Big Horn coal, this rate is of the order of 15×10^{-4} in/in/1,000 hrs. The axial strains represented by solid lines show some randomness from stress level to stress level, but in general exhibit behavior similar to that of Eagle coal of similar moisture content.

Test Series 12

This series consisted of 5 NX-size, uniaxially loaded specimens, incrementally loaded to detect possible creep at very high stress levels. Because the creep mechanism to be explored was envisioned to be moisture-independent, all specimens were sealed with Petrowax to inhibit moisture-induced time-dependent behavior. All five specimens, each in its own load frame, were loaded initially to 1,000 psi stress for 300 hours; the stress was then increased to 1,500 psi; after onset of stabilization of strains, the stresses were successively incremented by 200 psi until failure.

Fig. 3 shows the resulting creep curves for all specimens. The wax seals of Specimens 5 and 2 broke at 820 hours, and 1,100 hours, respectively, leading to subsequent high strain rates followed by spalling and failure. The stresses at that time were 1,700 and 1,900 psi, respectively, values well above the means for this coal observed in Series 11. Specimen 3 failed upon loading to 1,900 psi without having exhibited any prior increase in creep rate. Specimens 1 and 4 had been subjected to stresses up to 2,300 psi for a time of almost 2,800 hours without showing any creep

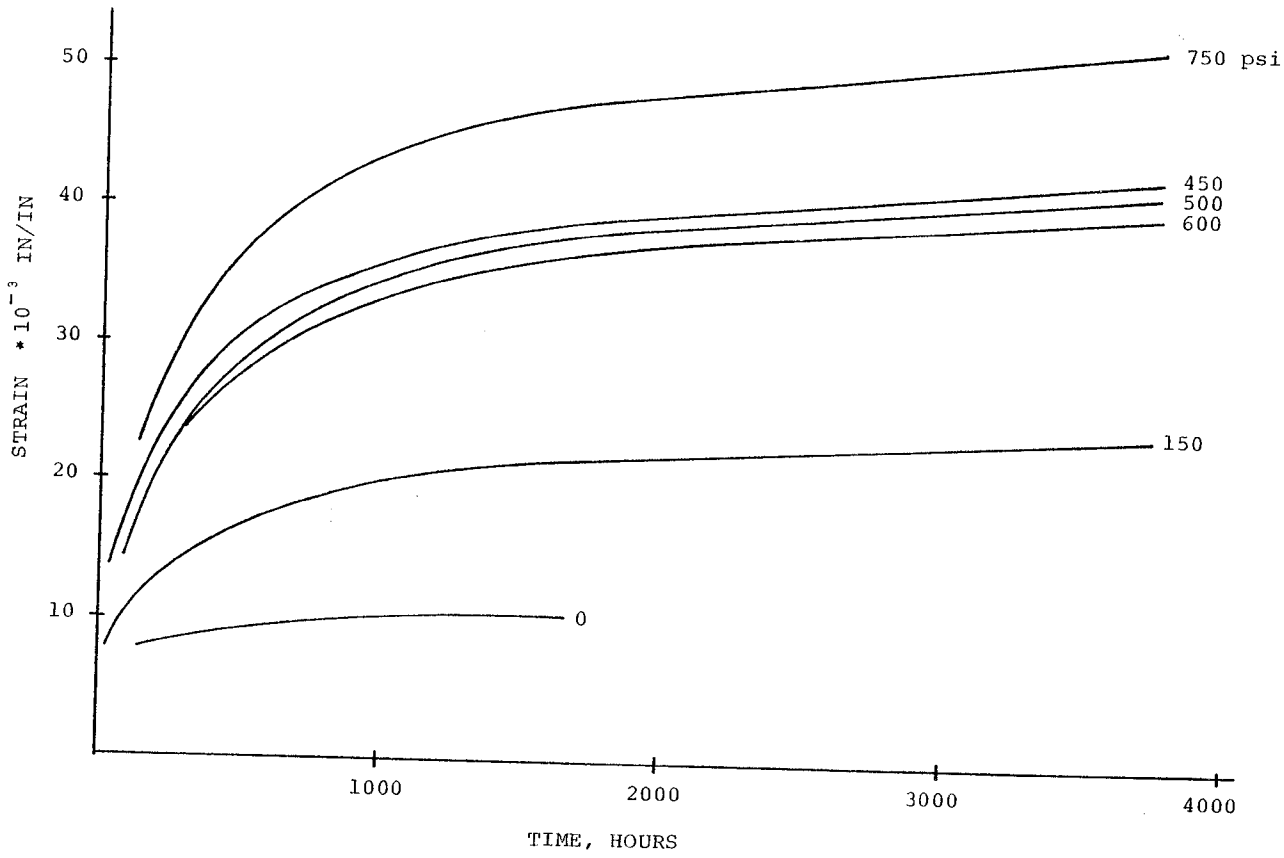

Figure 5.8 Creep Strain Curves for Big Horn Coal Test Series 11

instability. The test was terminated when the proving ring capacities of these load frames were exhausted.

It is concluded from this test series that no tertiary creep mechanism exists for Big Horn coal for any stress levels below its uniaxial strength.

Test Series 13

Test Series 13, consisting of five NX-size specimens of Eagle coal, had a purpose identical to that of Series 12: to detect the presence of a moisture-independent tertiary creep mechanism for this coal at high stress levels. To this end, all specimens were loaded incrementally, starting with a stress of 1,000 psi. Specimen 4 failed on first loading. Specimens 2 and 3 showed spalling and subsequent breakage of the wax seals during loading from 1,500 to 1,700 psi, leading to moisture loss followed by failure. No increase in creep rate was apparent until that time. A similar fate was suffered by Specimens 1 and 5 at 1,900 psi and 2,100 psi, respectively. In each case, no tertiary creep was apparent prior to loss of the moisture seal, thus confirming the findings of Series 12.

Test Series 14

Test Series 14 investigated methods of obtaining moisture drainage of coal specimens under sustained triaxial load in the Hoek cell. Comparisons were made between triaxial specimens and uniaxial test specimens. It was concluded that the moisture drainage and subsequent deformations of specimens were not equivalent between the triaxial and uniaxial test setups.

Test Series 15

Test Series 15 was composed of uniaxial tests on Paonia coal which provided information on a coal with a moisture content between 10 and 20 percent. Loading continued for 4,300 hours and then the specimens were unloaded and allowed to rebound for 1,500 hours.

Figure 5.9 shows the creep strain portion of the uniaxial test on each unsealed specimen. As in earlier creep tests, a stage of transient creep of about 2,000 hours is observed followed by a steady-state or linear creep regime. Above 3,500 hours, the creep rate of all specimens increased but because of premature termination of this test series it is unclear whether this behavior was due to the changes in the environment as noted earlier. Above 2,000 hours the sealed and unsealed behaved similarly, exhibiting negligible creep. The difference in creep strain between sealed and unsealed specimens is due to the initial, or transient creep of the unsealed specimens.

This observation leads to the surmise that two components are at work in time dependent deformation of coal: a transient stage associated with migration of moisture, and a secondary stage which is less dependent of moisture conditions, and might this be called steady state.

After approximately 4,300 hours of applying a uniaxial load to the samples of Paonia coal, the load was removed. The rebound of the samples with no axial load applied (except the heads to keep

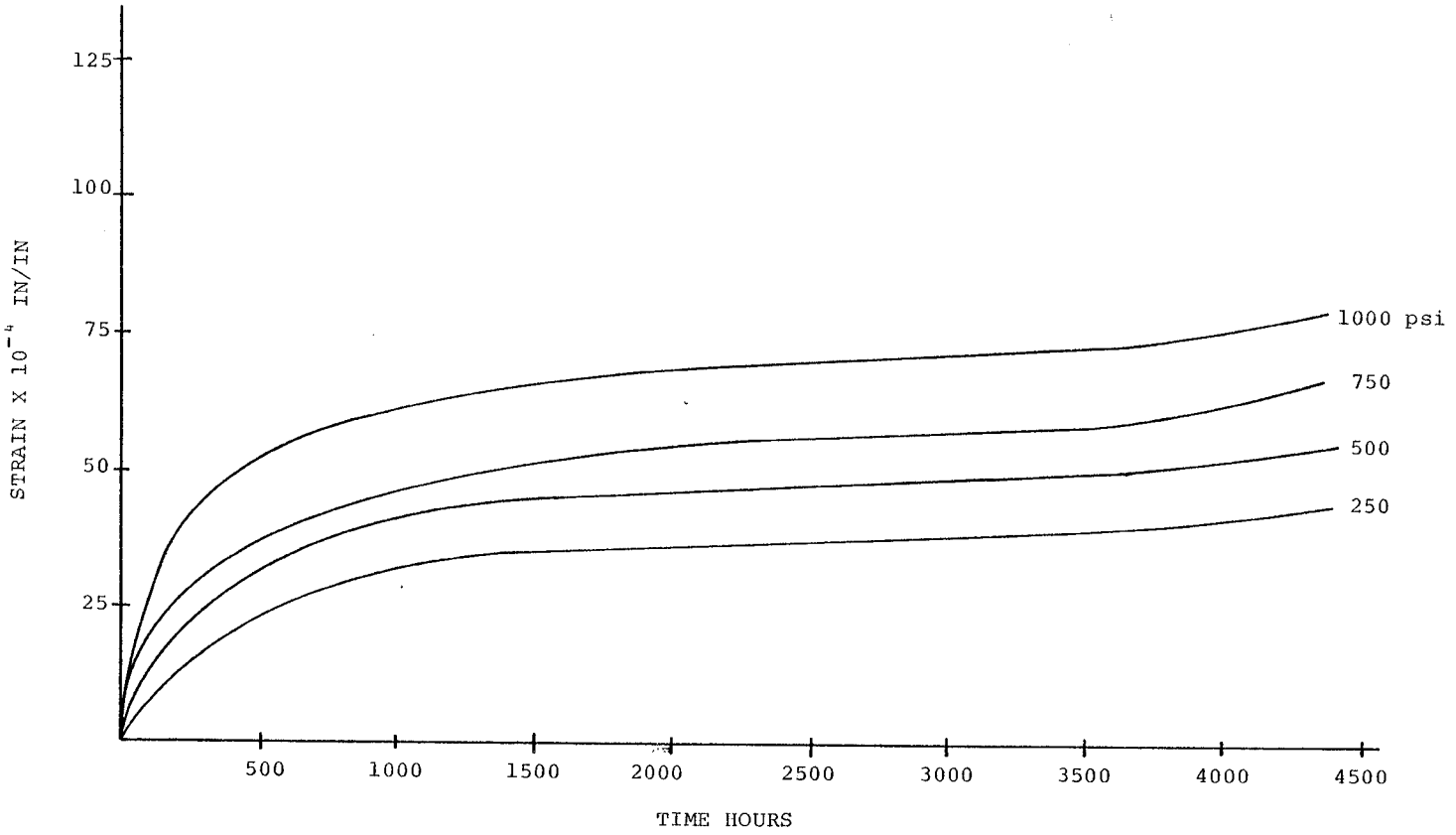

Figure 5.9 Time-Dependent Strain of Paonia Coal for Unsealed Samples

Test Series 15

the samples stationary) was observed for a further 1,150 hours. The results are shown in Fig. 5.10.

In all the samples there was a recovery of part of the strains induced by the loading. This rebound occurred for 300 hours (13 days) and then a leveling off of the strain rates occurred. After 300 hours the behavior of the samples was slightly erratic, but for the most part did approach steady state.

There appears to be no regular pattern to the amount of rebound of the Paonia coal after unloading. The sealed samples rebounded more than the unsealed samples. This was expected, since the unsealed samples experienced an irreversible moisture loss. Average values for the rebound from a given stress level would be difficult to predict since there was a large range of rebound for the samples tested, and no correlation between stress levels. All of the rebound curves have the same shape (see Figure 5.10). This shows that the time-dependent recovery of strains is not due to the applied stress level, but to the amount of time for which unloading is continued.

If the response of the 750 psi specimens is ignored, there is good correlation as to the amount of strain recovered instantaneously after the axial load is removed. The higher stress levels experienced more elastic rebound.

The time-dependent strain recovery appeared to be quite consistent. The average value of strain recoveries was 19% of the total strains experienced by the specimens.

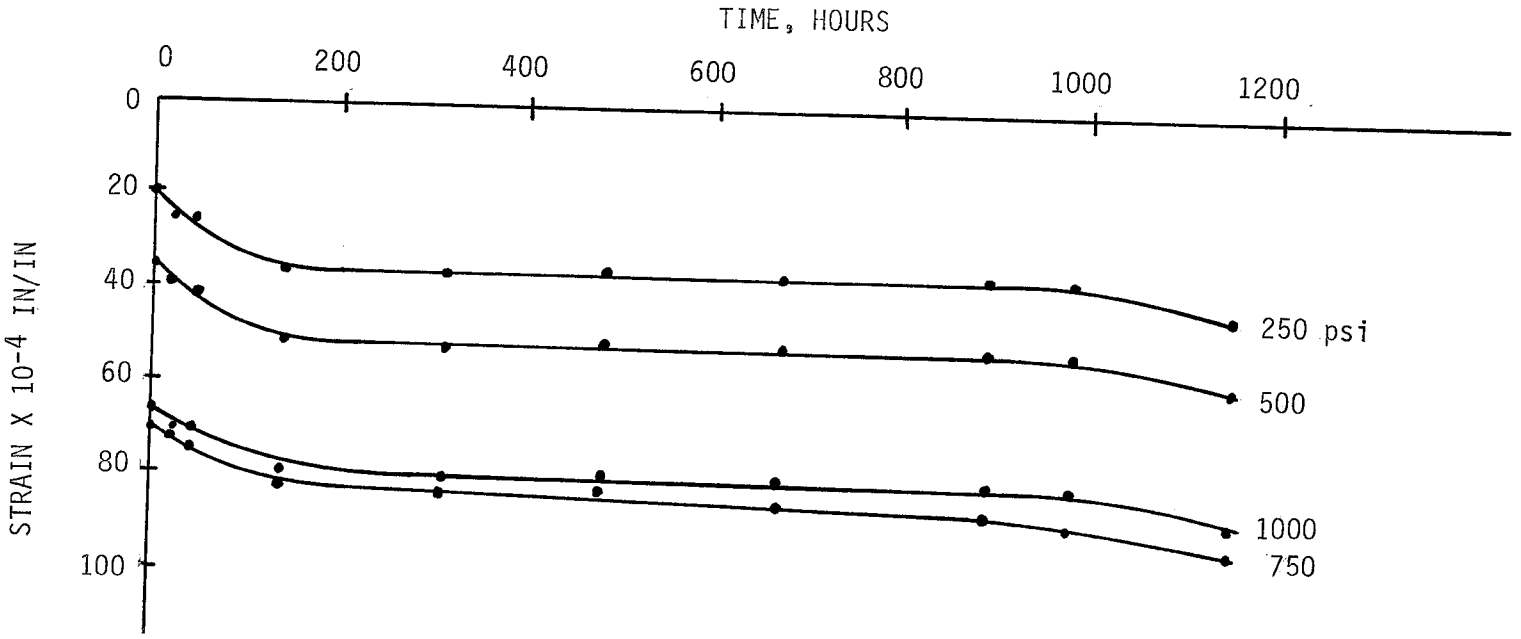

Figure 5.10 Unloaded Creep Curves for Paonia Coal-Unsealed Samples

Test Series 15

Test Series 16 and 17

The testing program of Series 16 and 17 was designed to test an alternate method of sealing samples and also to determine the effect of stress on Lincoln coal over a period of several hundred hours. To get a comparison of values for sealed specimens, an alternate to the Petrowax method was designed. The sample was enclosed in a rubber membrane which was then filled with water to stop any loss of moisture from the specimen. The samples behaved the same as the Petrowax sealed samples and showed no increase in strain with time. This rules out any possible consolidation process working on the internal structure of the coal. There was a slight decrease in strain for four of the five samples in the water bath. This can be accounted for by the fact that as the unsealed specimens strain, the stress level on the specimens decreases about 10 percent over a forty-eight hour period, and must be readjusted.

5.3 Summary

As mentioned before, the range of moisture contents for the coals tested provides an opportunity to examine the full range of moisture in relating creep of coal to moisture content. Accordingly, Fig. 5.11 shows selected creep curves of coals of various moisture content. It is seen that all the data fits the picture well, and reinforces the earlier conclusion that the effect of stress level becomes more pronounced for moister coals.

A different way of representing the effect of coal moisture on creep is shown in Fig. 5.12, which plots the creep strain versus

Coal	Moisture Content
Pittsburgh (pi)	2.6%
Raton (R)	2.9%
Paonia (P)	11.6%
Eagle (E)	27.7%
Gillette (G)	34.7%

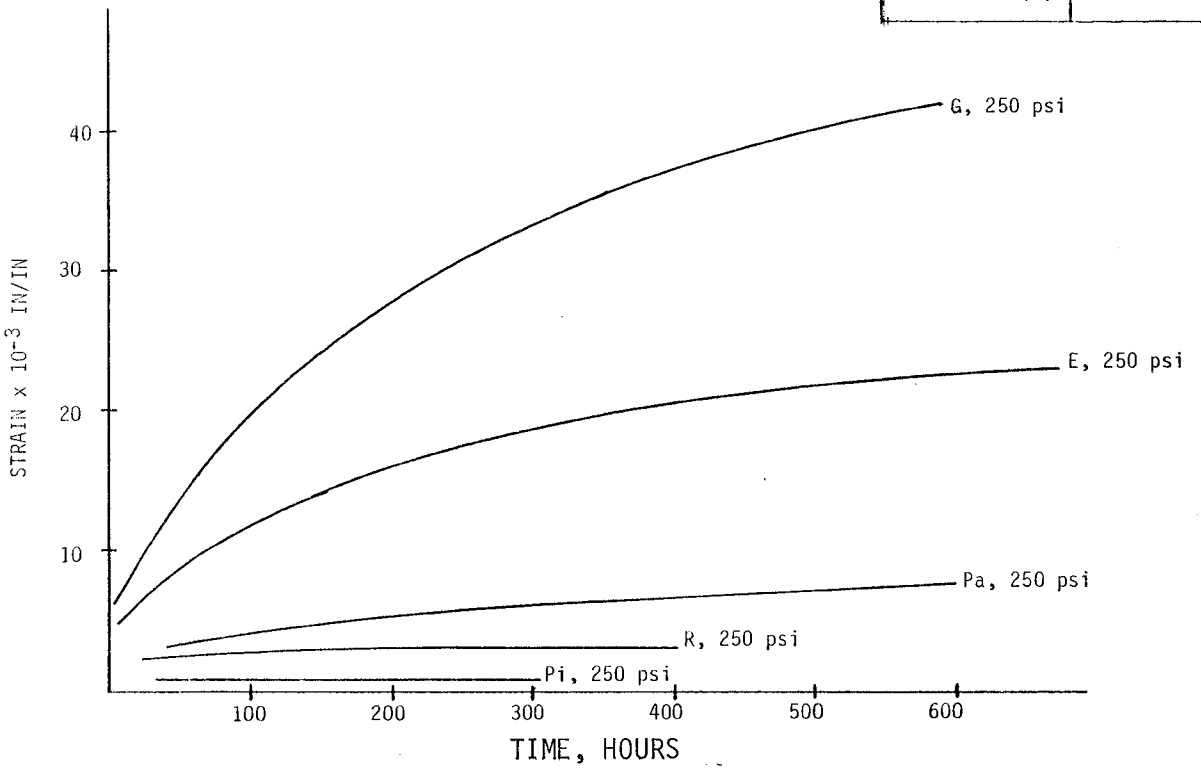

Figure 5.11 Creep of Coals with Different Moisture Contents

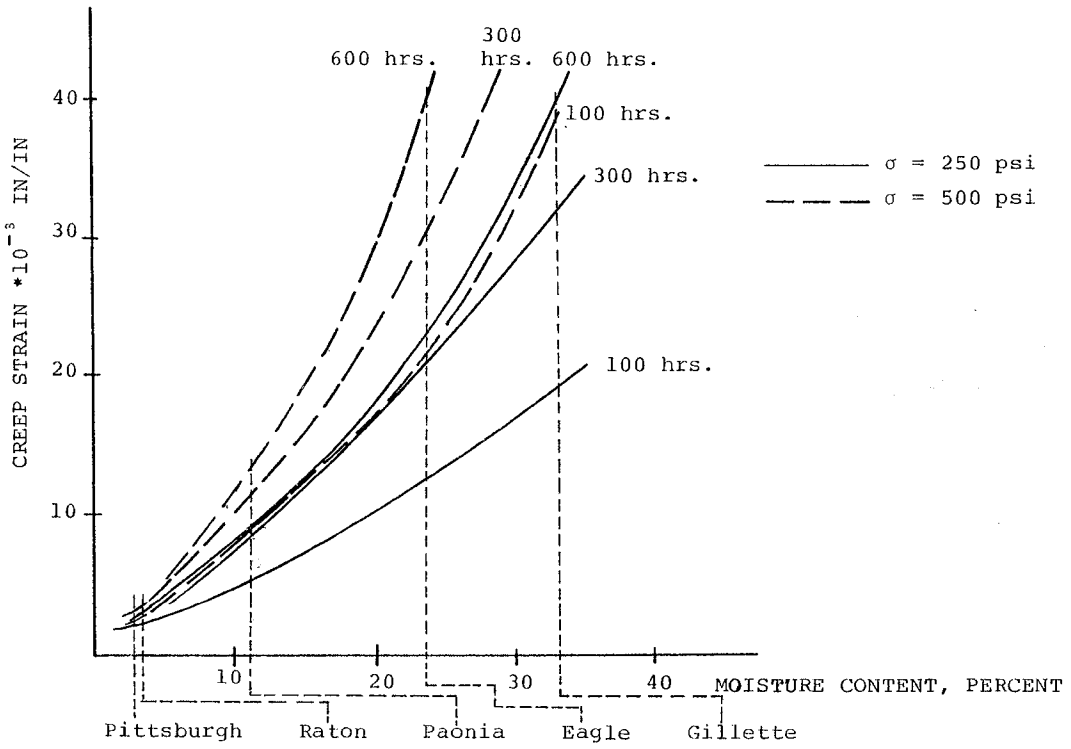

Figure 5.12 Relation of Creep Strain of Coal to Initial Moisture Content

moisture content, with stress level and time as parameters. The response of five coals is prominently shown, and indicates that the creep strains for coal are much lower for dry coals than for moister coals. Indeed, it appears from this plot that creep of such magnitude that it might be of engineering significance occurs only in coal of moisture content above 15 or 20 percent.

CHAPTER 6

CREEP BEHAVIOR

6.1 Introduction

In Chapter 1 a review of existing creep laws to represent the behavior of rocks in uniaxial compression was presented. However, much of the work done was not based on the actual phenomenon of the internal structure, but on empirical formulations that provided the best fit to experimental data. Any physical model based on the behavior of coal will become quite complex as shown by Kidybinski (1966). Some simplifications can be made in the models to get acceptable solutions.

There are several well recognized characteristics of the creep behavior of rock. When a compressive stress is applied to a creep specimen, an elastic strain occurs instantaneously. As the specimen is kept under stress a time-dependent deformation or creep occurs at a rate that is variable depending on time, stress, and environmental conditions. At any point in time the elastic strain can be immediately recovered by removing the compressive stress. The time-dependent deformation can be divided into three stages. In the initial stage creep behavior is transient with a decreasing creep rate. This is followed by a period of deformation where the creep rate is constant. In the final stage the strain rate increases and the specimen eventually fails by

excessive deformation. The idealized creep curve is shown in Fig. 6.1 This chapter is concerned with the first two stages of creep behavior. In coal the observed response under sustained loading has been discussed in Chapter 5. It was concluded that the time-dependent response of coal can be broken down into several components; elastic strain, shrinkage strain and creep strain. Fig. 6.2 shows the relationship between these three strains for a coal material. Figure 6.3 shows the relationship between the three strain components for a typical rock material and can be compared to Fig. 6.2.

Cracks and Pores

Coal contains both macroscopic and microscopic cracks. For most coals there are two systems of oriented macroscopic cracks, known as cleats. The planes of the two cleats are roughly perpendicular to the bedding plane and the angle between the two cleat planes is usually 90^{o}. These crack systems are most likely due to changes in tectonic stresses during the history of the deposit. There are also randomly distributed cracks of macroscopic and microscopic sizes.

The internal structure of coal is highly porous. The pore sizes range down to tens of angstroms.

Modes of Fracture Due to Creep Testing

Long term uniaxial compression tests on coal have revealed that there are three modes of fracture that can develop as shown in Fig. 6.4 a, b, c (Sture, 1976). Fig. 6.4a shows a multifracture

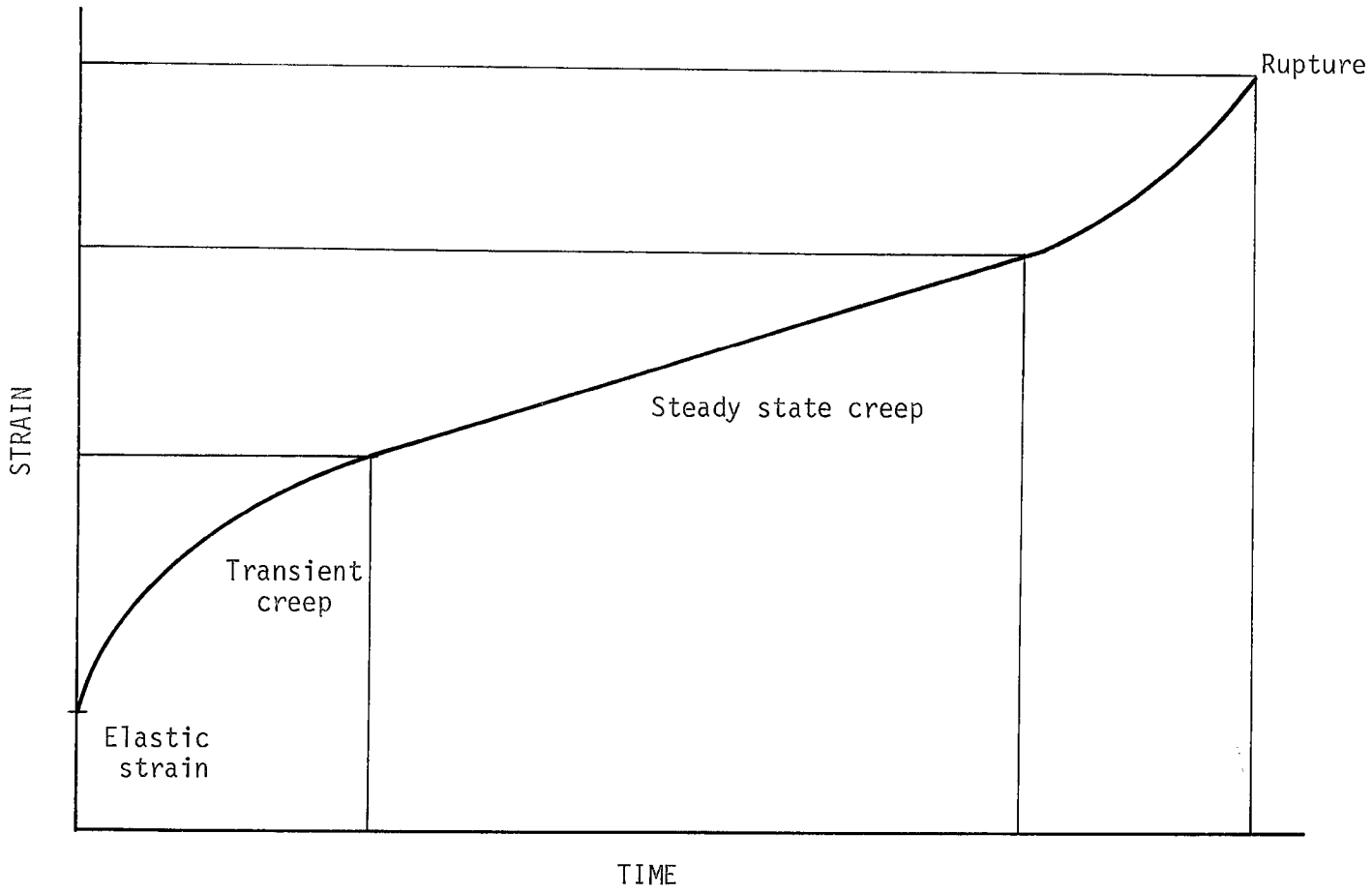

Figure 6.1 Idealized Creep Curve for a Rock Material

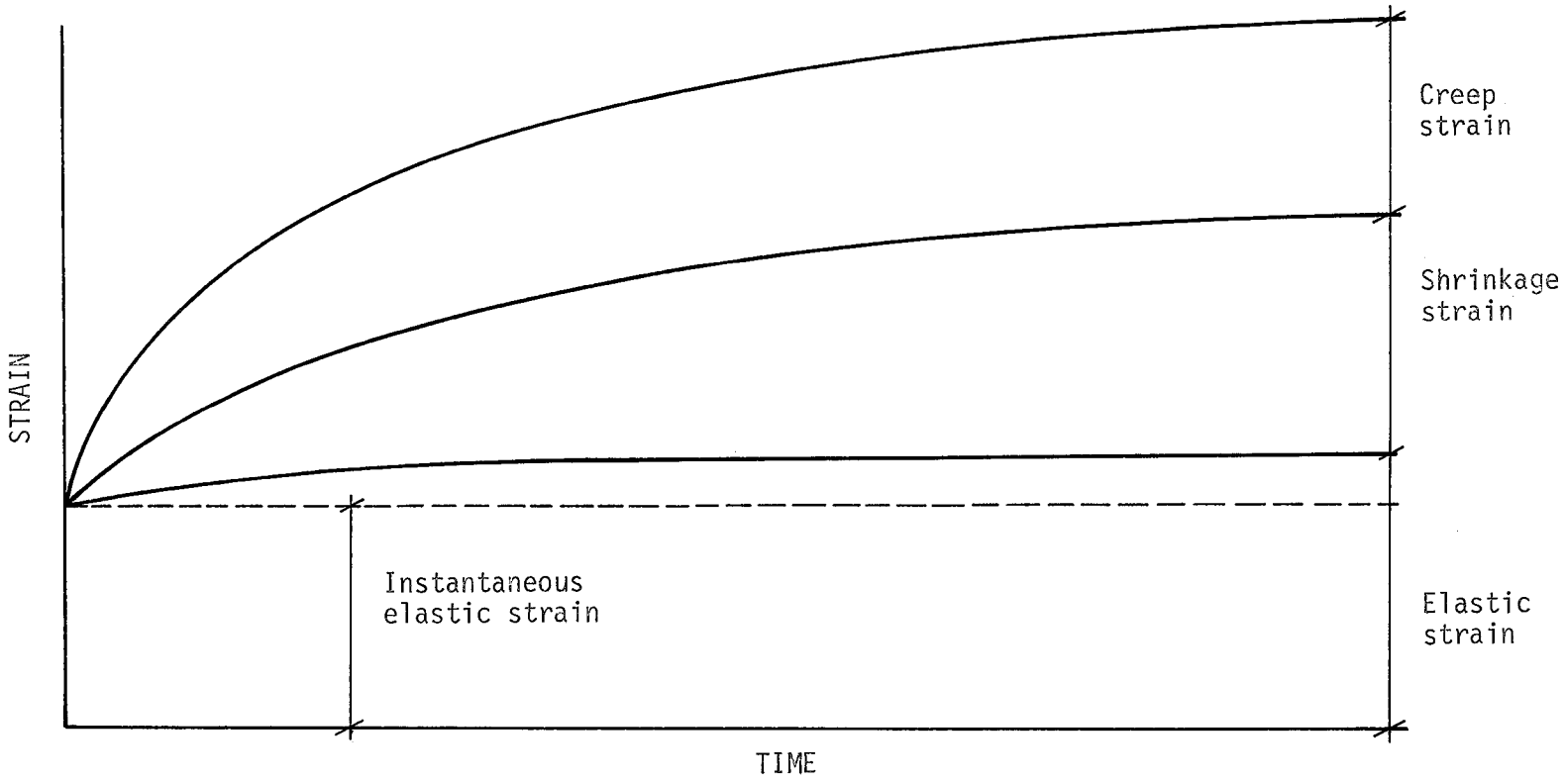

Figure 6.2 Time-Dependent Strain of a Loaded and Drying Coal Specimen

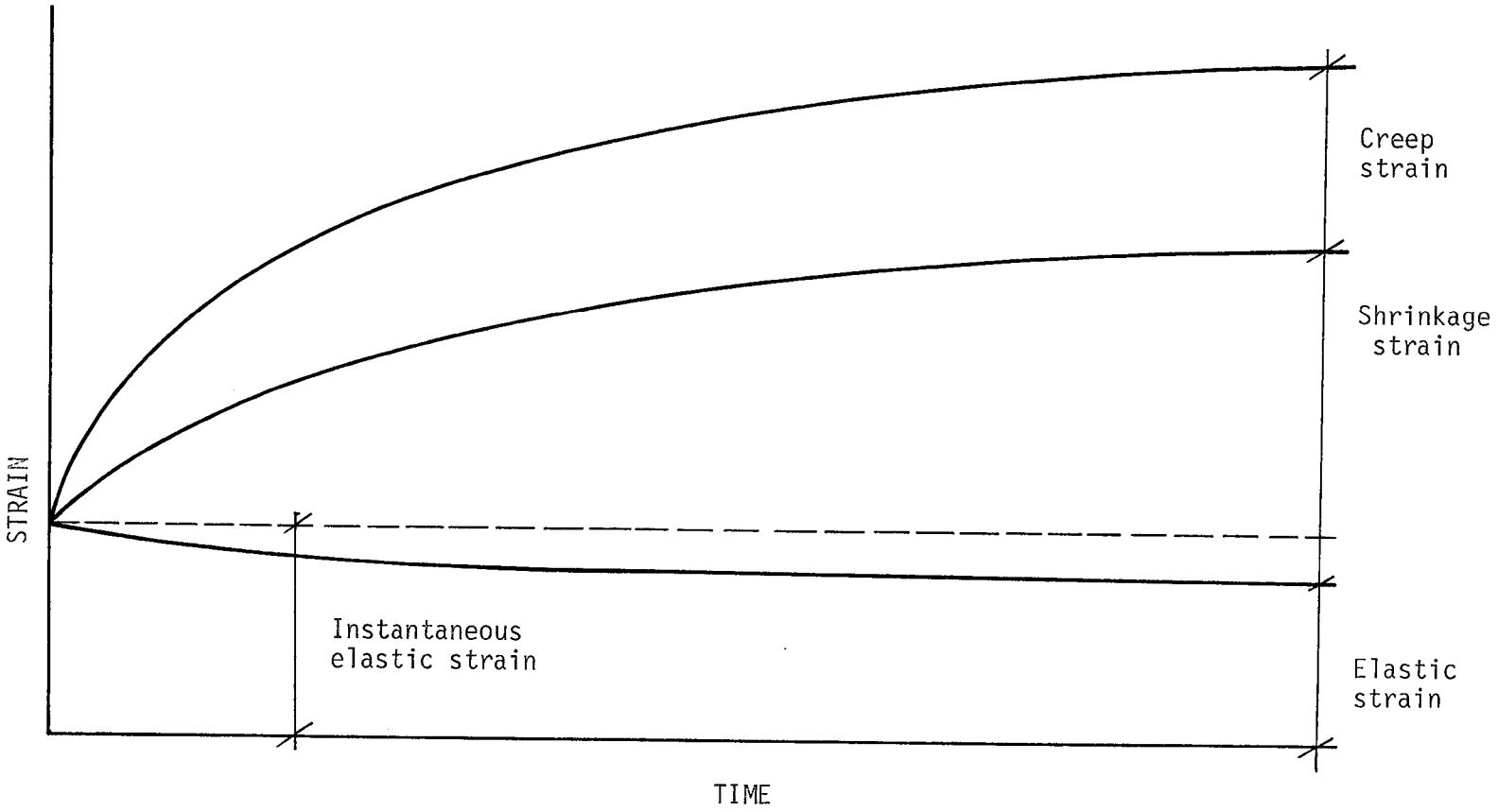

Figure 6.3 Time-Dependent Strain of a Loaded and Drying Rock Specimen

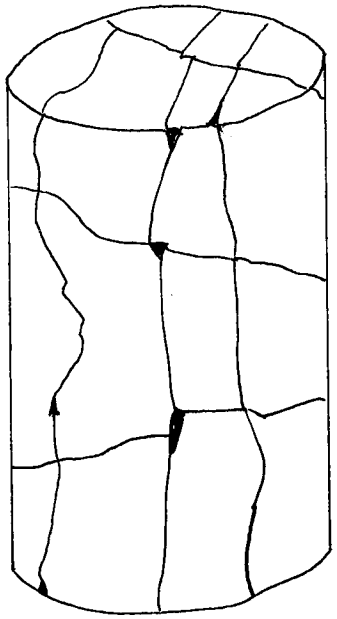

(a) Multifracture

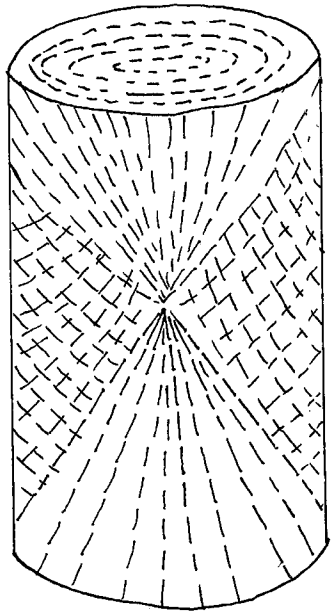

(b) Shearfracture, complete development

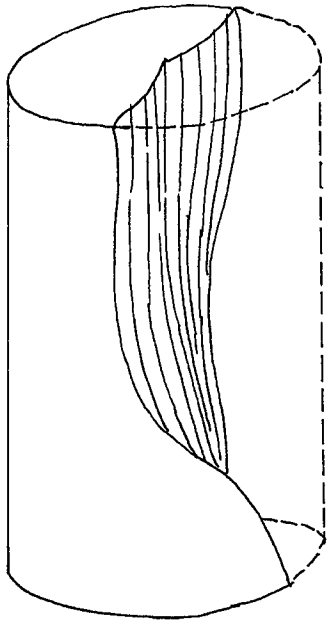

(c) Monofracture

Figure 6.4 Modes of Fracture in Coal

which was caused by the existence of microcracks throughout the specimen. A major set of fractures run almost parallel to the direction of the principal compressive stress, and a second set of fracture planes runs normal to the first set. Since all of the samples are oriented with γ=0, these two fractures planes represent the major and minor cleats. Fig. 6.4b represents an ideal shear fracture throughout the specimen. This mechanism occurs in ductile rocks where the inelastic flow is characterized by the theory of plasticity. This mode of fracture commonly occurred in the cyclic saturation tests.

The third mode of fracture as shown in Fig. 6.4c is described as monofracture. Monofracture is characterized by small microcracks along a plane of fracture. The increase of tensile stresses, caused by external loads and internal pressures, on the crack tips of the propagating plane of fracture creates a large fracture plane parallel to the direction of the major principal compressive stress. This mode of fracture was observed in dry coal after creep testing had progressed for several thousand hours.

6.2 Empirical Modeling

The question as to whether creep of rock materials is better analyzed by a logarithmic law or a power law is difficult to answer, but has some significant practical implications. If the mechanism of creep deformation is considered as progressive dislocation and transverse sliding within and between mineral constituents of rock, and if temperatures are low and the stress

level is well below the instantaneous fracture level, dislocation and sliding will begin only at the weaker points in the material. However, as deformation increases, the resistance will become greater as progressively stronger energy barriers must be overcome. A strain hardening causes the deformations to continue but at a decreasing rate. A logarithmic creep description may then be approximate.

If temperatures and stresses are higher it is possible to overcome the build-up of resistance due to strain hardening and the dislocations and slip planes "pile up" on one another in quick succession. If this occurs, the strain hardening effect that helped procuce the logarithmic creep law is partially lost. Then a power law can more accurately describe the creep behavior.

The only empirical modeling of creep strain done during the Bureau of Mine sponsored project, "Constitutive Relations of Coal and Coal Measure Rocks," was performed by Tulin (Chapter 6, Ko and Gerstle, 1976). He developed several expressions based on exponent or power laws to describe the creep strain-stress-time response of Eagle coal. The time domain was divided into three periods, short term creep, less than 30 days; intermediate creep, less than 100 days; and long term creep, more than 100 days. By plotting the data on log-log scales of creep strain vs. time and making corrections for erratic data, straight and parallel lines were obtained for each stress level in the region of long term creep. A curvilinear relation was found in the region of

intermediate and short term creep. This curvilinear region is referred to as Region 1 and the linear region as Region 2. Both regions were best described by the equation

$$e = ct^q \sigma^p \tag{6.1}$$

where

e = creep strain

t = time, days

σ = stress, psi

c = coefficient to be determined

q,p = powers to be determined

Three simultaneous equations were solved for each time region, using different known values of strain, time and stress level. The equations which give the most accurate results are listed below.

$$\text{Region 1} \quad e = 8.42 \times 10^{-3} t^{0.35} \sigma^{0.13} \quad ; \; t<100 \tag{6.2}$$

$$\text{Region 2} \quad e = 17.51 \times 10^{-3} t^{0.195} \sigma^{0.13} \quad ; \; t>100 \tag{6.3}$$

However, no generality can be attributed to the exponents or to the other coefficients as material properties.

6.3 Rheological Modeling

Introduction

A numerical and analytical study of the results of a series of creep tests run on coal is presented in this section. Several models are proposed along with coefficients to match the experimental data. The models are based on the rheological interpretation of the natural process. The initial model is designed as a

Kelvin-Voigt element with a strain-dependent spring added in parallel. Modifications are then made in the initial model to get a second model that gives a better correlation with the experimental curves. Numerical techniques are used to solve the governing differential equations obtained from the models. Predicted curves are then compared with the experimental creep response curves. The adjusted experimental curves and the curves from the second model compare favorably. All experimental data used are from tests run on the Eagle Mine coal (Series 3, 4, 5 and 8 as described in Chapter 5).

The predicted curves are based on different stress levels. There are other factors that affect the creep response as much as varying stress levels. The moisture content of the coal and the moisture environment that the test is run in both affect the creep response. The random variation of the coal tends to give a scattering of results that adds to the difficulty of response prediction. There is a definite relation between stress levels and creep. This is the only variable considered in this section. Humidity is held constant for all tests. An average of data values from the different series of tests is used to obtain an adjusted set of data.

The creep response is broken down into two distinct sections, a nonlinear phase and a linear phase. The initial phase is nonlinear and occurs until 2,000 hours. This phase shows some of the characteristics of consolidating soil and hence guides the

choice of the rheological model. The second phase is a linear response which occurs above 2,000 hours and is not considered in this section.

Experimental Results

The experimental data is obtained from test Series 3, 4, 5 and 8 (Chapter 5) run on coal samples from the Eagle Mine, Weld County, Colorado. The specimens were all oriented with their axes perpendicular to the bedding plane. Tests were conducted at five stress levels; 250, 500, 750, 1,000 and 1,250 psi in uniaxial test frames.

The test series from the Eagle Mine are used since they provide the most uniform and systematic response of any test series run during the project. The results of several tests from each stress level are used. The results at each stress level are averaged to determine the averaged actual creep response of that level as in Fig. 6.5. The values of the instantaneous elastic strain and the value of the strain due to moisture shrinkage (S = 0 psi) are subtracted from each stress level. Between 0 hours and 400 hours there are inconsistencies in the relative magnitudes of stress levels. These are changed so a more systematic response is obtained for the adjusted curves of Fig. 6.6. At the two highest stress levels, 1,000 and 1,250 psi, there are incomplete results so curves are extrapolated to the adjusted curves in Fig. 6.6. The justification for adjusting the experimental data is that the fracturing and non-uniformity of the samples produced large variations in the response from sample to

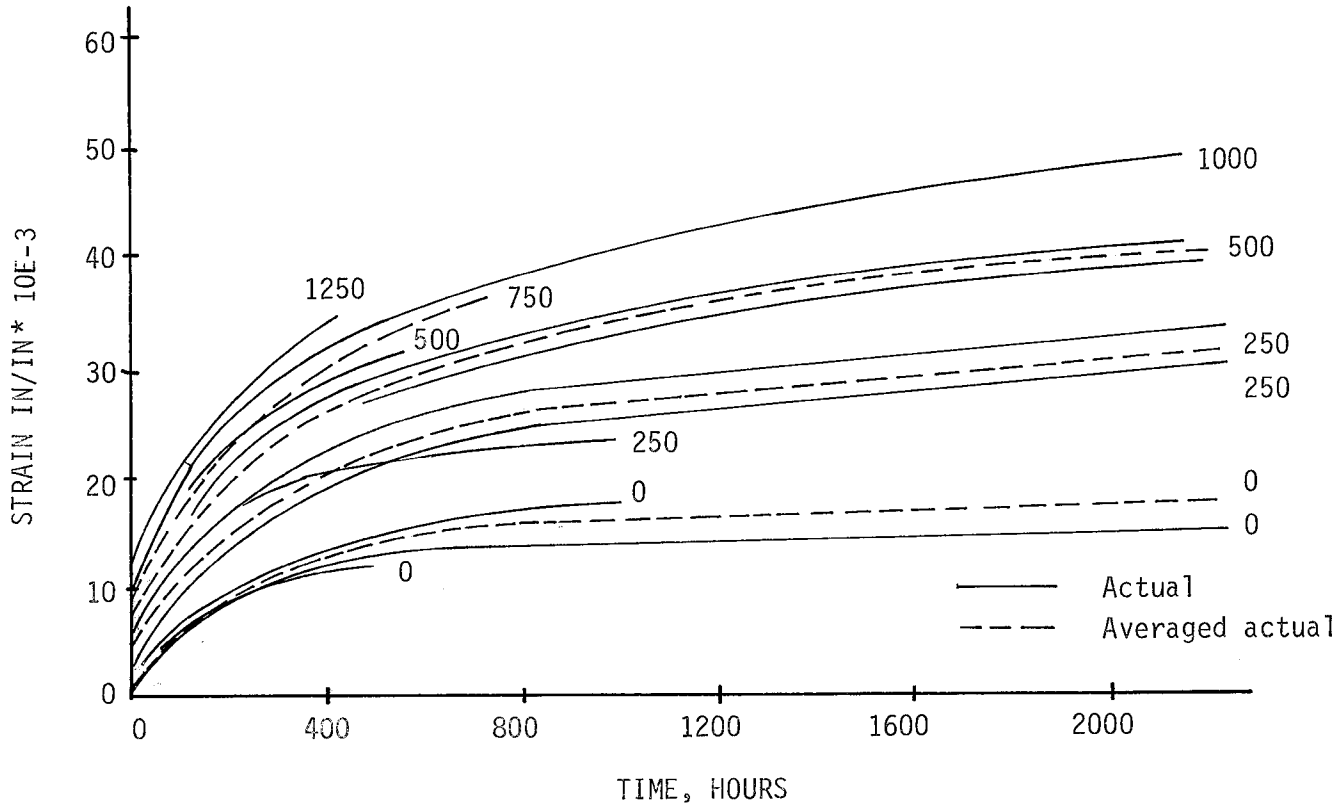

Figure 6.5 Summary Curves Eagle Coal

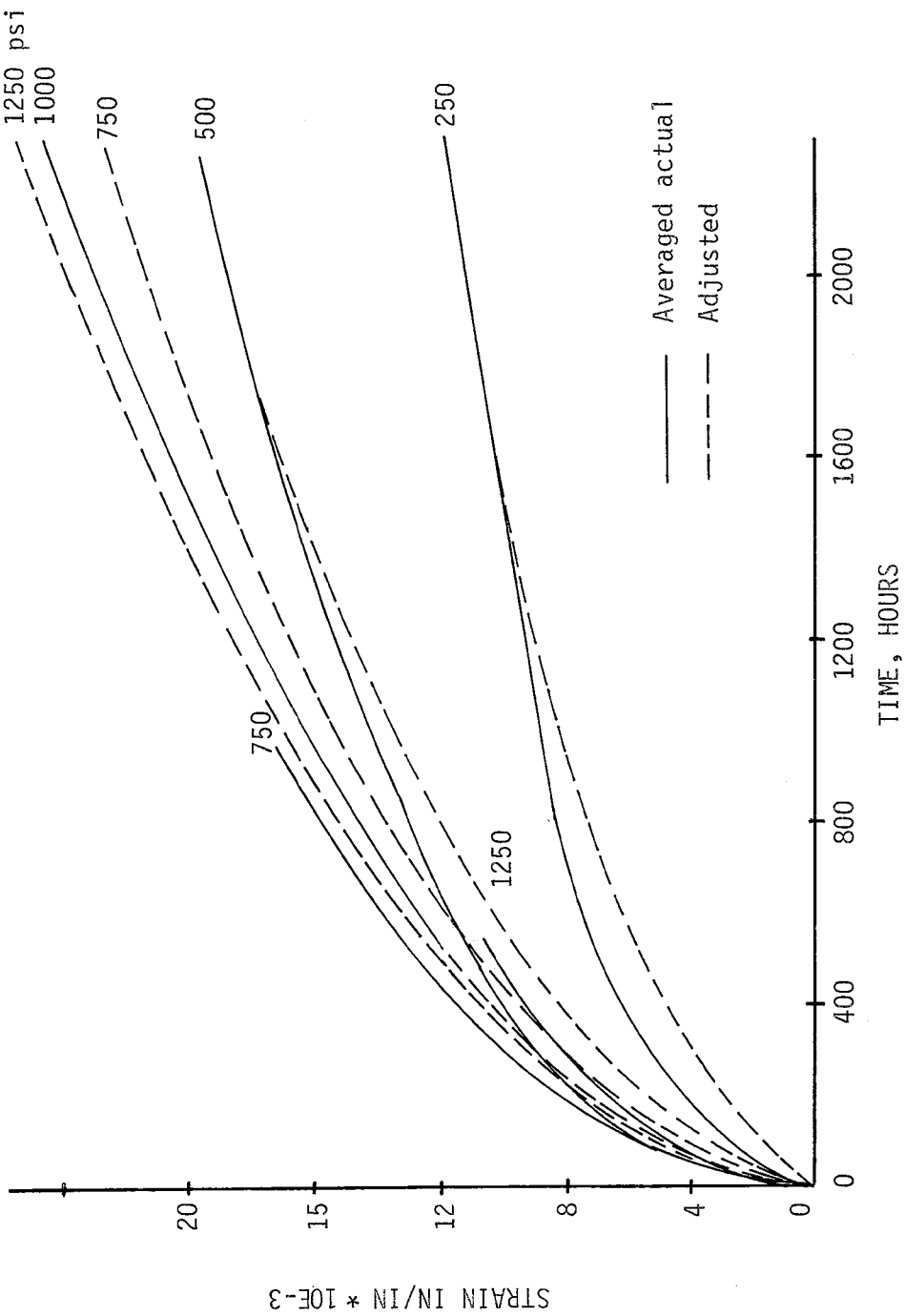

Figure 6.6 Averaged Actual and Adjusted Creep Strain Curves, Eagle Coal

sample. An attempt was made during the actual testing to use totally continuous coal samples, but the samples still were not uniform. The adjustments made were meant to produce an internally consistent set of experimental data.

Analytical Approach

From the physical properties of coal a rheological model is designed to describe the response of a particular series of creep tests on coal. By examining the creep curves it can be seen that the material is becoming stiffer from the decreasing strain rate. There is also a high degree of nonlinearity exhibited by the decreasing distance between successive stress levels. These factors will necessitate the development of a nonlinear rheological model. The physical basis of this model is a structure of particles that are separated by voids. As a stress is applied, the particles rearrange themselves, decreasing the void space and increasing the coherence between particles (Fig. 6.7). The rearranging of the particles causes a stiffening

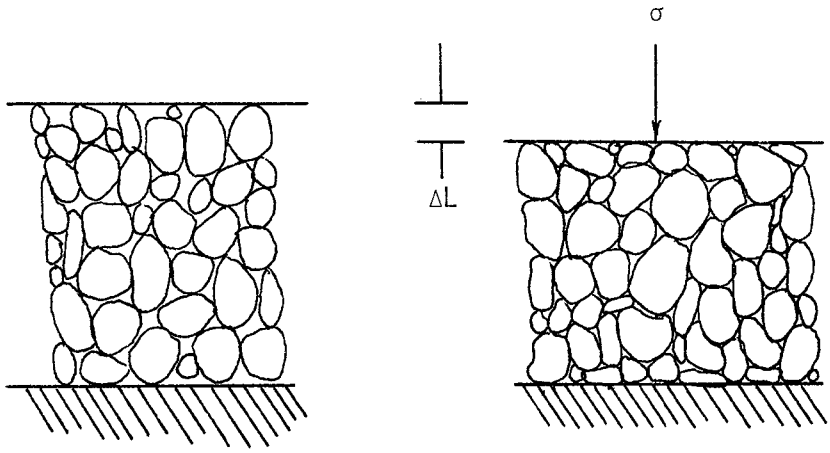

Figure 6.7 Physical Interpretation of Process

of the material. The proposed model is based on the Kelvin Voigt rheological model as shown in Fig. 6.8.

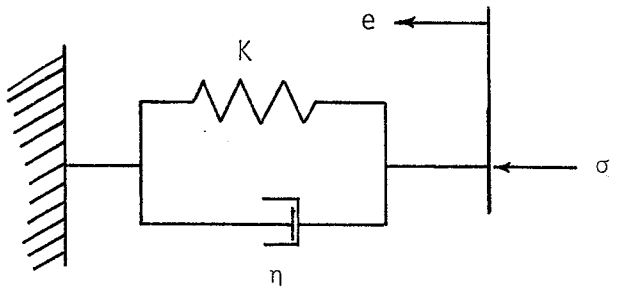

Figure 6.8 Kelvin Voigt model

For the model of Fig. 6.7 the behavior is represented by

$$\frac{de}{dt} + \frac{ke}{\eta} = \frac{\sigma}{\eta} \tag{6.4}$$

where the spring stiffness K is constant.

However, the postulated inter-pore behavior shown in Fig. 6.7 indicates that the stiffness should depend on the strain. In the model the spring stiffness K must be related to the strain. It is proposed that the stiffness term be dependent on the instantaneous elastic strain and the creep strain. The strain due to drying shrinkage is subtracted out from creep curves and not considered in the stiffening of the coal. If the stiffness of the material K increases linearly with respect to the strain experienced by the coal a relationship as shown in Fig. 6.9 is obtained. To make the relationship more nonlinear the stiffness can be related to a power of the strain. To match the form of the creep curves a power of between zero and one must be used.

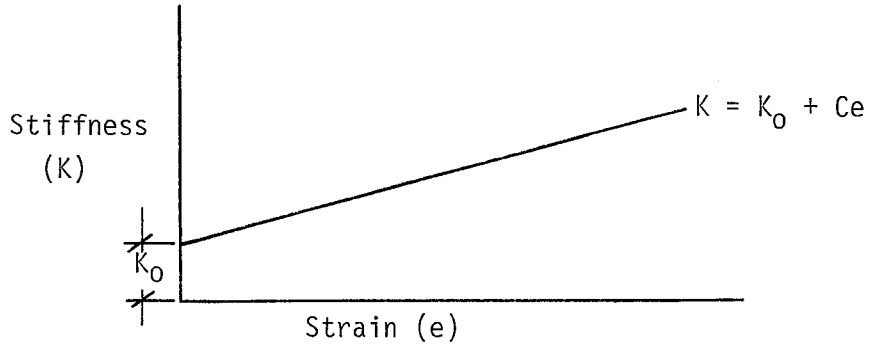

Figure 6.9 Relationship of Stiffness Increasing Linearly with Respect to Strain

Figure 6.10 shows this proposed stiffness to strain relationship. The governing differential equation using a stiffness term as

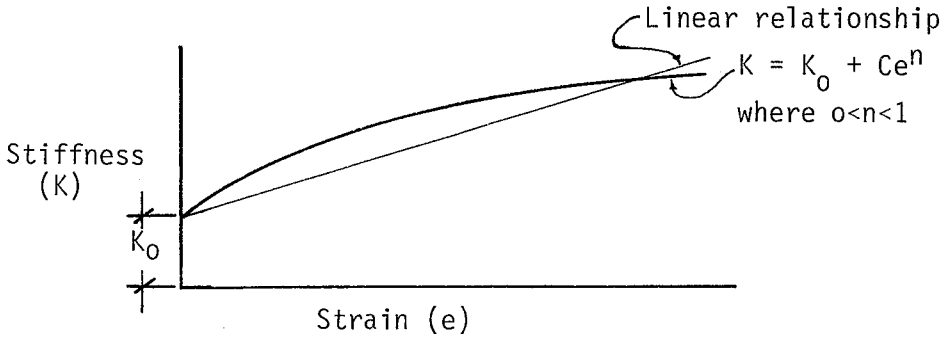

Figure 6.10 Relationship of Stiffness to a Power of the Strain

shown in Fig. 6.10 is obtained as

$$\frac{de}{dt} + \frac{(K_o + C_e n)}{\eta} e = \frac{\sigma}{\eta} \qquad (6.5)$$

or by generalizing, combining coefficients, and solving for $\frac{de}{dt}$ the following equation is obtained

$$\frac{de}{dt} = C_3\sigma^q - (C_1 e\sigma^P + C_2 e^r) \qquad (6.6)$$

where

$q = 1$

$p = 1$

$1<r<2$

The first term is the initial rate term and the last two terms are the decreasing rate terms.

There is no analytical solution to this differential equation. A numerical technique is therefore adopted to solve the governing equation. The Runge-Kutta Method is used because of its versatility. This piecewise linear technique for nonlinear differential equations is sufficiently accurate and fast enough for this application.

By substituting into Equation 6.6 three different strain rates corresponding to three stress levels, three algebraic equations are obtained which contain C_1, C_2, C_3, q, p and r as unknowns. The values of q, p and r are set at unity and then the initial values for C_1, C_2 and C_3 are obtained by solving the three simultaneous equations. Exact values for C_1, C_2 and C_3 are then found by trial and error and comparison with experimental curves. The value of r from one to two does not seem to affect the shape of the curve to any extent. The values of q and p remain at one for this model.

The most accurate curves derived from this model, as shown in Fig. 6.11 still do not give a reasonable prediction when

compared with experimental curves over the whole range of time and stress levels.

The predicted curves in Fig. 6.11 show several characteristics of the experimental curves. There is a convergence of the strain response as the stress levels increase. The basic shape of the curve is obtained; however, the shortcomings of the model are also apparent now. The initial rate of the prediction curves is directly proportional to the stress level, whereas in the experimental data the initial rates are closer to each other in magnitude. For example, the initial rate $\frac{de}{dt}0$ is equal to the term $C_3\sigma$. This means that $\frac{de}{dt}0$ at 1,250 psi is five times as great as $\frac{de}{dt}0$ at 250 psi. However, the experimental results show that $\frac{de}{dt}0$ at 1,250 psi is approximately twice $\frac{de}{dt}0$ at 250 psi. Another problem encountered is the continuing decrease in the rate after 1,250 hours. From the experimental data an almost constant rate is found at all stress levels above 1,250 hours. It is not possible to find values of C_1 and C_2 which will produce an almost constant rate (except 0) for the strain response above 1,250 hours.

With the above considerations a second model is proposed that is more empirical in nature, but based on the same differential equation. Only two changes need be made in the equation from experience gathered on the first model. The second model is set up as:

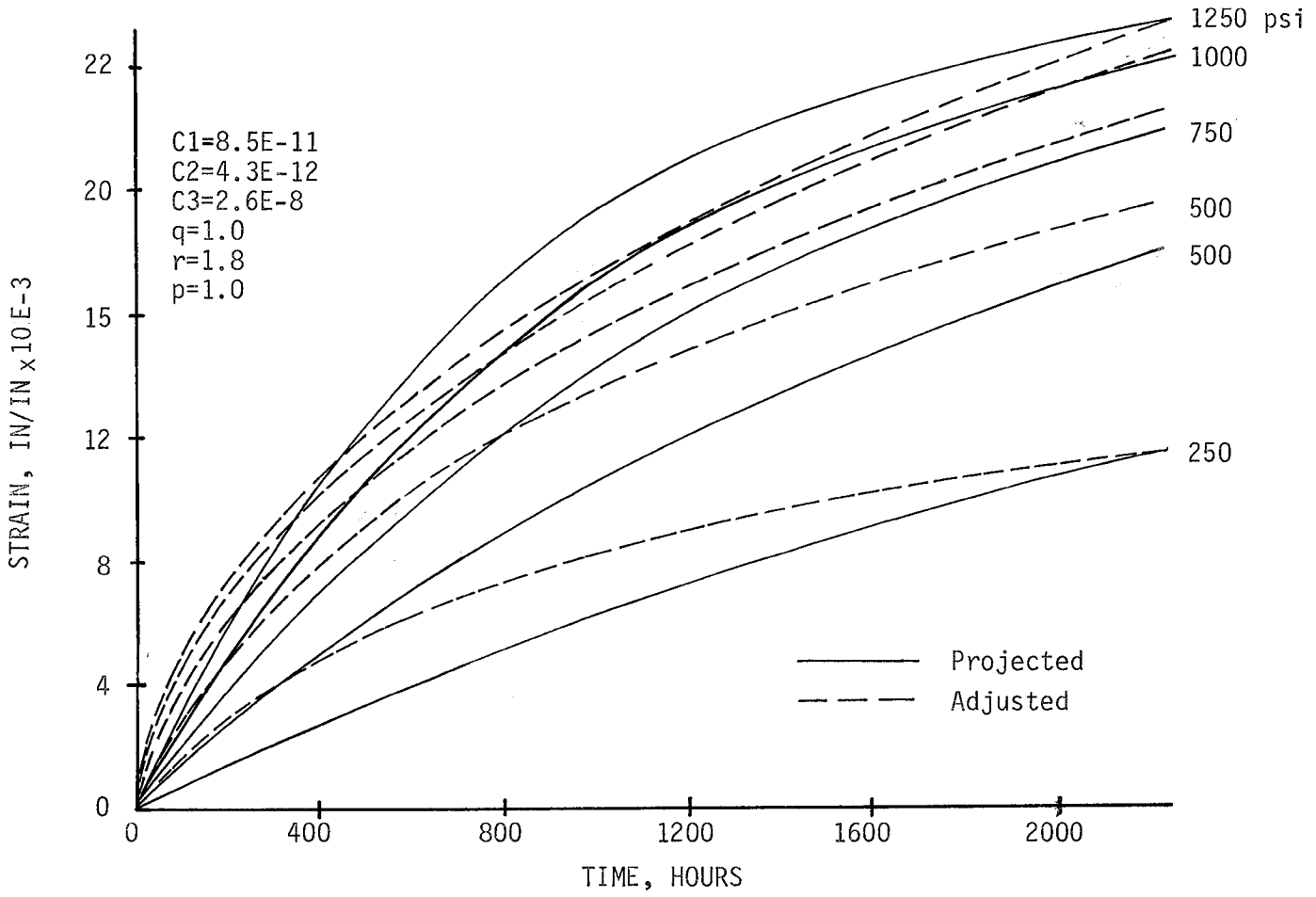

Figure 6.11 Numerical Analysis of Creep Response Model 1

$$\frac{de}{dt} = C_3\sigma^q - (C_1\sigma^p e + C_2 e^r) \qquad (6.7)$$

where

$0<q<1$

$p = -1$

$1<r<2$

By varying q the initial rates can be made almost equal, better predicting the experimental results. A value of $q = 0.3$ produces the best grouping of initial rates as shown in Fig. 6.12. To accomplish this, the reciprocal of σ has to be used in the first rate decreasing term. This is due to the lesser rate decrease at higher stress levels. From the first model $C_1\sigma e$ at 1,250 psi was greater than $C_1\sigma e$ at 250 psi when it should be the opposite inequality. Hence, $C_1\sigma^{-1} e$ will produce a better fitting curve. The second model, as shown in Fig. 6.12, predicts the experimental curves quite well for times greater than 1,000 hours.

With the use of rheological models it is possible to find an approximate solution to nonlinear creep response at varying stress levels. However, this is only a simplified model to represent a complex process. It does appear that the factor of material stiffening with increasing strain is a governing variable in the final solution of creep response.

The second model proposed more as an empirical correlation corresponds well to the adjusted experimental data. There is,

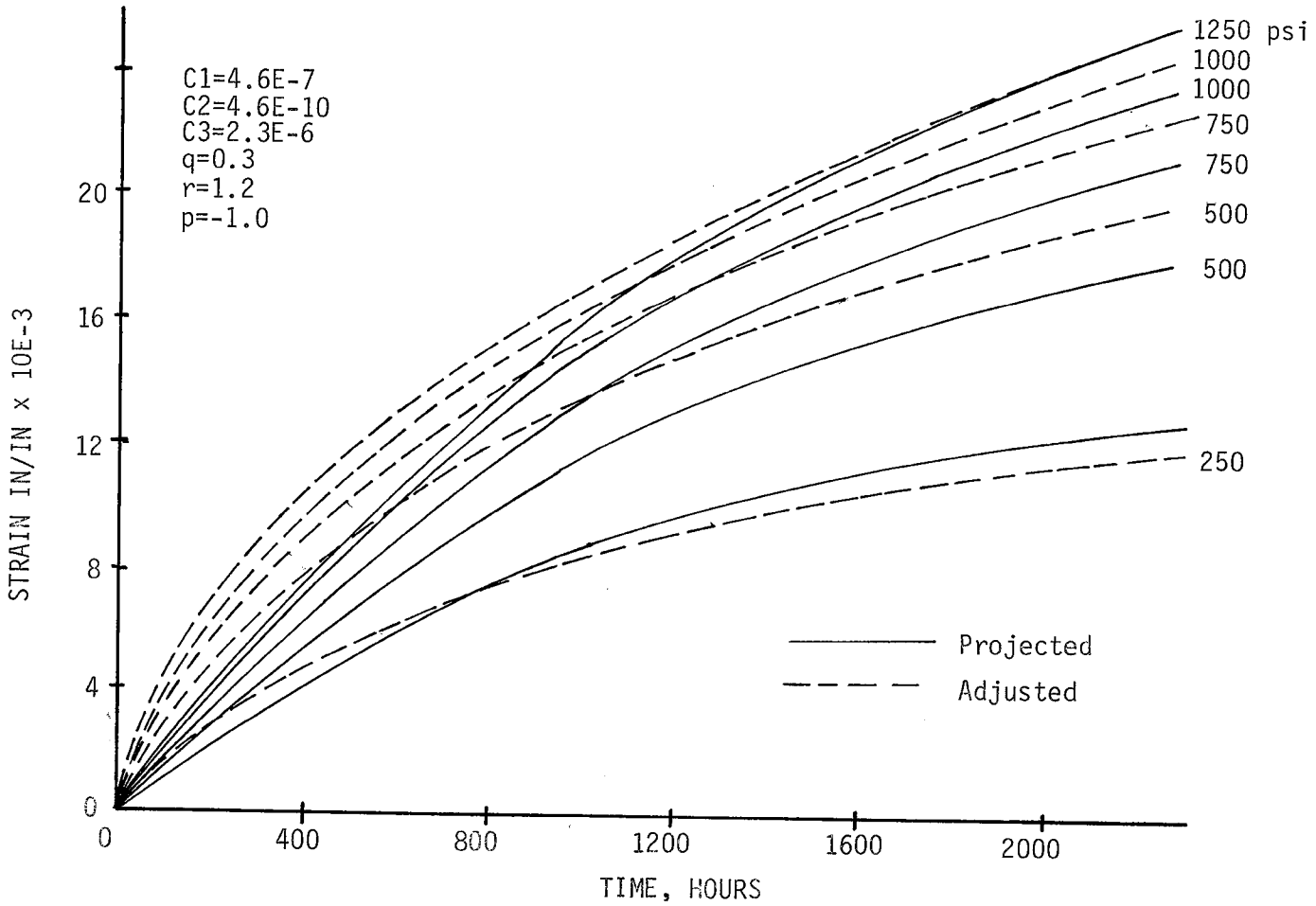

Figure 6.12 Numerical Analysis of Creep Response Model 2

however, a range of strain values for each stress level from the different series of tests on the same Eagle coal. This can account for a 20 percent variation in the experimental values from the predicted values.

CHAPTER 7

SUMMARY, CONCLUSIONS, AND RECOMMENDATIONS FOR FUTURE WORK

7.1 Summary

In this thesis two phenomena have been investigated, 1) drying shrinkage of coal, and 2) creep behavior of coal. With respect to these investigations the following has been accomplished.

1. A survey of previous work done on shrinkage and creep was presented to provide background information and justification for the ensuing work.

2. Theories of partial saturation, capillary tension, effective stress and delamination were proposed to explain the behavior of coal due to moisture migration.

3. Testing was performed to validate proposed theories of drying shrinkage in coal.

4. Creep testing was performed to obtain a large base of data relating different independent variables to each other and to time dependent strain.

5. Comparisons of existing empirical expressions to describe creep were discussed and their deficiencies pointed out.

6. A rheological model of creep behavior was formulated and compared with actual creep strain data.

7.2 Conclusions

The uniaxial testing of the time-dependent response of coal has provided conclusive results. Time-dependent strain has been observed and analyzed due to both drying shrinkage and applied external stresses.

The drying shrinkage of coal was of the same order of magnitude as the strain due to applied stresses. The drying shrinkage of each coal type was highly dependent on the insitu moisture content and the relative humidity of the environment. By decreasing the relative humidity from 95 percent to 20 percent, the strain increased by roughly six times. The strain could be stopped or reversed in uniaxially tested specimens by either coating the samples in impermeable wax or submerging them in a water bath. These effects became more pronounced for the coals with higher initial moisture content. By cycling the saturation of coal specimens a hysterisis of strain was obtained. This led to progressive failure after several cycles.

The creep behavior of coal (the part which is independent of moisture migration) is a complex phenomenon. It was difficult to isolate each independent variable to obtain meaningful test results. Many experimental curves were obtained for coals from Eagle, Big Horn, Lincoln, and Orchard Valley mines. Lesser amounts of data were obtained for coals from Federal #1 and York Canyon mines mainly due to the low moisture content that made time-dependent strain almost negligible. The response of coal to various stress levels was highly nonlinear. For this reason

a nonlinear rheological model was designed. Coefficients were obtained to match one set of consistent experimental data from Eagle coal. The advantages and disadvantages of different types of empirical modeling were discussed and it was concluded that a power law could best be used to describe creep over time periods of practical interest.

As coal is mined from a seam using the room and pillar method a large amount (up to 60%) of the coal must be left to support the new openings. If the time dependent strength and deformation properties of the coal pillars can be more exactly determined, extraction ratios can be increased with less conservative designs.

By testing coal specimens in a uniaxial test frame, an approximation of the conditions in the pillar is duplicated. Stress and environmental conditions can be varied just as they are in a mine. However, due to the large natural variations in the properties of coal even within one seam exact values of strength and time-dependent strain may be difficult to predict. A more acceptable solution in the light of all the testing that has been performed is to specify a range of strengths and time-dependent strains based on the existing data.

The data that has been obtained and the correlations that have been made are a result of combining experimental results with both an empirical and analytical approach. Deficiencies were found in both types of analysis. The main problem is that the coal material does not behave as a linear visco-elastic material

and must be analyzed as being nonlinear. Most existing work on time-dependent strains of rocks, however, is based on empirical formulation.

7.3 Recommendations for Future Work

Work done up to this point has been concerned with obtaining material response to varying conditions of applied stress and moisture migration.

Future work should be directed to applying the obtained relations of strain and time to actual insitu conditions. Coal mine openings could be modeled for time-dependent behavior. In this way predictions could be made as to deformations and failures over long periods of time.

Insitu testing could be run to determine the relationship of laboratory behavior of coal to the behavior of coal in mine openings. This, however, would involve complicated measurements and the introduction of many uncontrollable variables. Probably the most useful insitu testing would be to vary the environment of the mine opening and measure deformations and stresses.

Computer modeling of mine openings could be performed, as mentioned in the introduction, to calculate the moisture flow and ensuing deformations. This would require the use of either a theoretically based model of time-dependent behavior or empirically obtained correations.

By monitoring the response of the openings over a period of time and comparing with the numerical predictions, a validation of the material properties used in the analysis could be obtained.

REFERENCES

1. Andrade, E. N. (1910), Viscous Flow in Metals. Proceedings of the Royal Society, Vol. A94, No. 1.

2. Colback, P. S. and B. L. Wiid (1965), "Influence of Moisture Content on the Compressive Strength of Rocks", Proceedings of the 3rd Canadian Rock Mechanics Symposium, Toronto, Canada, pp. 69-83.

3. Cruden, D. M. (1971a), "Creep Law for Rocks Under Uniaxial Compression", International Journal of Rock Mechanics and Mining Science, Vol. 8, pp. 105-126.

4. Cruden, D. M. (1971b), "Single-Increment Creep Experiments on Rock Under Uniaxial Compression", International Journal of Rock Mechanics and Mining Science, Vol. 8, pp. 127-142.

5. Dragowski, A. (1970), "An Analysis of Rock Deformations Due to Swelling and Shrinkage", Proceedings of the 2nd Seminar on Soil Mechanics and Foundation Engineering, Lodz, pp. 369-386.

6. Griggs, D. T. (1939), "Creep of Rocks", Journal of Geology, Vol. 47, p. 225.

7. Handin, J., R. V. Hager, Jr., M. Friedman, and J. N. Feather (1963), Experimental Deformation of Sedimentary Rocks Under Confining Pressure: Pore Pressure Tests, Bulletin Am. Assoc. Petroleum Geologists, Vol. 47, pp. 717-755.

8. Hardy, H. R. (1965), Inelastic Behavior of Geologic Materials-I, Divisional Report FMP 65/155-P, Mines Branch, Ottawa, Canada.

9. Haroon, M. (1974),"Hysteresis Affected Shrinkage and Rheological Behaviour of a Drying Soil-Cement Slab", Ph.D. Thesis, University of Mississippi.

10. Hudel, P. P. and N. Sitar (1975), "Effect of Water Sorption on Carbonate Rock Expansivity", Canadian Geotechnical Journal, Vol. 12, No. 2, pp. 179-186.

11. Kioybinski, A. (1966), "Rheological Models of Upper Silesian Carboniferous Rocks", International Journal of Rock Mechanics and Mining Science, Vol. 3, pp. 279-306.

12. Ko, H. Y. and K. H. Gerstle (1974), "Constitutive Relations of Coal", Report USBM Grant No. GD110894, University of Colorado.

25. Price, N. J. (1964), "A Study of Time-Strain Behavior in Coal Measure Rocks", International Journal of Rock Mechanics and Mining Science, Vol. 1, pp. 277-303.

26. Skempton, A. W. (1961), "Effective Stress in Soils, Concrete and Rocks", Pore Pressure and Suction in Soils, Butterworths.

27. Sture, S. (1976), "Strain-Softening Behavior of Geologic Materials and its Effect on Structural Response", Ph.D. Thesis, University of Colorado.

28. Terry, N. B. and W. T. A. Morgans (1958), "Studies of the Rheological Behaviour of Coal", Proceedings of the Conference on Mechanical Properties of Non-Metallic Brittle Materials, London, Butterworths, p. 239.

29. Terzaghi, K. (1943), Theoretical Soil Mechanics , John Wiley and Sons, Inc., New York.

30. U.S. Coal Mine Production by Seam (1975, 1976), Keystone Coal Industry Manual, McGraw-Hill, New York.

31. Van Eeckhout, E. M. and S. S. Peng (1972), "The Effect of Humidity on the Compliances of Coal Mine Shales", International Journal of Rock Mechanics and Mining Science, Vol. 12, pp. 335-340.

32. Wiid, B. L. (1970), "The Influence of Moisture on the Pre-Rupture Fracturing of Two Rock Types", Proceedings of the 2nd Congress of the International Society of Rock Mechanics, Vol. 2, pp. 239-244.

33. Winkel, B. V., K. H. Gerstle, and H. Y. Ko (1972), "Analysis of Time-Dependent Deformations of Openings in Salt Media", International Journal of Rock Mechanics and Mining Science, Vol. 9, pp. 249-260.